DAVIDSON LABORATORY

REPORT 1115

STEVENS INSTITUTE
OF TECHNOLOGY

CASTLE POINT STATION
HOBOKEN, NEW JERSEY

HYDROFOIL FLUTTER PHENOMENON AND
AIRFOIL FLUTTER THEORY
Vol. III, Sweep and Taper

by

Charles J. Henry

and

M. Raihan Ali

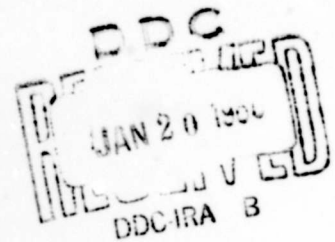December 1965

HYDROFOIL FLUTTER PHENOMENON AND AIRFOIL FLUTTER THEORY
Vol. III, Sweep and Taper

by

Charles J. Henry

and

M. Raihan Ali

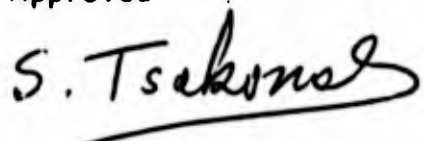Approved

S. Tsakonas

S. Tsakonas, Chief
Fluid Dynamics Division

ix + 34 pages
4 tables, 16 figures
1 appendix (2 pages)

ABSTRACT

Measured decay rates and flutter speeds for a two-degree-of-freedom hydrofoil model with sweep or taper do not agree with the decay rates and flutter speeds predicted by two-dimensional strip theory, whereas the measured and predicted frequencies are in agreement. Calculations based on the two-dimensional strip theory show that increasing sweep angle or decreasing taper yields higher flutter speeds as well as higher values of the critical density ratio. It is shown that flutter-speed predictions based on quasi-steady representations of the unsteady hydrodynamic forces are not valid.

KEYWORDS

Hydroelasticity
Flutter

TABLE OF CONTENTS

BLANK PAGE

NOMENCLATURE

A	span to semichord ratio $= s/b_o$
A_1, B_1, C_1	parameters defined in Equation (30)
A_r, B_r, C_r, D_r, E_r, F_r	parameters defined in Equation (33)
A_0, A_1, A_2, A_3	parameters defined in Equation (36)
$a(y)$ $b(y)$	distance from midchord to rotational axis, positive if the rotational axis is aft
$b(y)$	local semichord length
b_0	reference semichord length
$C(k)$	Theodorsen function defined in Equation (15a)
$e(y)$ $b(y)$	distance from y-axis to rotational axis, positive if the rotational axis is aft
F	a real constant
$F(k)$, $G(k)$	real and imaginary parts of $C(k)$, respectively
$F(y,t)$, $T(y,t)$	lift and moment per unit span, respectively, relative to the y-axis
F_h, F_α, T_h, T_α	harmonic hydrodynamic derivatives defined in Equation (27)
$f_j(x,y)$	j^{th} displacement mode shape
$g_j(y)$	j^{th} spanwise mode shape
$\dot{H}(y,t)$	downwash velocity at 3/4 chord point, defined in Equation (40)

$h(y,t)$, $\alpha(y,t)$ translational and rotational displacements, respectively, for two-dimensional airfoil section

h_0 initial value of h

i $\sqrt{-1}$

K_1, K_2 translational and rotational spring stiffnesses, respectively

k reduced frequency

k_0 reduced frequency at $b = b_0$

$L(y,t)$, $M(y,t)$ lift and moment, respectively, per unit span in two-dimensional flow

L_h, L_α, M_h, M_α two-dimensional harmonic hydrodynamic derivatives

$M_{j\ell}$ generalized mass defined by Equation (3)

$m(y)$ mass per unit span

n number of displacement mode shapes

p Laplace transform variable

$\Delta p(x,y,t)$ load distribution on lifting surface

P, Q, R parameters defined in Equation (33)

$Q_j(t)$ generalized force defined in Equation (4)

$q_j(t)$ generalized coordinate in j^{th} displacement mode shape

r number of translation mode shapes

$r_\alpha b$ radius of gyration per unit span about rotational axis

s	span length of model
T	taper ratio
$T(t)$	time dependence of hydrofoil displacement
t	time
U	forward speed of hydrofoil
U_f	forward speed at flutter
x, y	orthogonal Cartesian coordinate system in plane of lifting surface
$x_\alpha b$	distance from rotational axis to center of gravity, positive if center of gravity is aft
$Z(x,y)$	space dependence of hydrofoil displacement
Λ	midchord sweep angle
μ	density ratio
μ_{CR}	critical density ratio
ρ	fluid density
$\varphi(t)$	Wagner function given approximately by Equation (41)
Ω_j	dimensionless natural frequency defined by Equation (48)
ω	response frequency
ω_j	uncoupled natural frequency in j^{th} mode
ω_f	response frequency at flutter

BLANK PAGE

INTRODUCTION

In two earlier hydroelastic investigations at the Davidson Laboratory, measured flutter speeds of several hydrofoil models were compared with flutter speeds predicted by airfoil flutter theory. The hydrofoil models considered in those studies were highly simplified, to provide the best possible basis for corroboration of the theory. In particular, they were constrained to motions in only two degrees of freedom, namely, uniform translation and rotation; and they were mounted between large end plates, to insure two-dimensional flow. These models were tested over a range of density ratio[1] and center-of-gravity location,[2] while other parameters, such as rotational-axis location, natural-frequency ratio, and radius of gyration, were held constant.

The dynamic response characteristics of the experimental setup (i.e., decay rate and frequency, as well as amplitude ratio and relative phase of the responses in the two degrees of freedom) were compared with those predicted over a range of speeds by two-dimensional unsteady airfoil theory. The results show that the theory overestimates the decay rate near the critical value of density ratio, leading to a non-conservative prediction of flutter speed in the range of density ratio which is of interest for hydrofoils. Thus it was concluded that, for deeply submerged hydrofoils with two degrees of freedom and in two-dimensional flow, aero-elastic theory can be used only as an indication of the proximity of an actual flutter boundary. Flutter tests must be carried out for accurate predictions of flutter speeds, when flutter is imminent.

Other investigators have encountered this discrepancy.[3,4,5,6] None of the proposed explanations[3,4] has, however, been substantiated. To study the physical mechanism leading the discrepancy, reliable flow studies and force measurements, at high values of reduced frequency $(.3 < k < 2)$, are needed.

The scope of the hydroelastic studies at the Davidson Laboratory has been extended in subsequent investigations to include the effects of

operation near a free surface [7,8,9] and more realistic support conditions. [10]

The comparison of measured and predicted flutter speeds is extended in the present study to include the effects of planform variations (particularly sweep and taper) with the same basic two-degree-of-freedom system as that described in the first two volumes relating to this series of investigation. [1,2] Measured flutter speeds are compared, in this report, with flutter speeds predicted by the two-dimensional stripwise technique.

It has been suggested by several investigators that a simplified, quasi-steady representation of the unsteady hydrodynamic forces might be used to predict the flutter speed of hydrofoils. [11,12] To shed further light on such an approach, this report also presents several comparisons of the flutter-speed predictions based upon quasi-steady and unsteady representations of the hydrodynamic forces.

Computations were carried out at The Computer Center of Stevens Institute of Technology, which is partly supported by the National Science Foundation.

THEORETICAL ANALYSIS

INTRODUCTION

The hydrofoil, because it is relatively thin and has small values of camber and angle of attack, is replaced by a lifting surface* with no thickness which has the same shape as the hydrofoil in planform and front elevation. The unsteady motion of the hydrofoil is then presumed to consist of small perturbations normal to the lifting surface, since other motions do not have an appreciable effect on lift. Furthermore, it is assumed that the motion can be represented by a finite sum of prescribed displacement mode shapes, each multiplied by an unknown time-dependent amplitude. Thus, for the case of a flat lifting surface in the x-y plane, the normal displacement $Z(x,y)T(t)$ is represented by

$$Z(x,y)T(t) = \sum_{j=1}^{n} f_j(x,y) \, q_j(t) \tag{1}$$

where $f_j(x,y)$ are the mode shapes, n is the number of modes, and $q_j(t)$ are generalized coordinates giving the amplitude of displacement in each mode as a function of time t.

The equations of motion for the hydrofoil can be written as[13]

$$\sum_{\ell=1}^{n} M_{j\ell} \, \ddot{q}_\ell(t) + \omega_j^2 M_{jj} q_j(t) = Q_j(t) \quad ; \quad j = 1, 2, \ldots, n \tag{2}$$

where $M_{j\ell}$ is the generalized mass, ω_j is the uncoupled natural frequency of oscillation in the jth mode, and $Q_j(t)$ is the generalized force. In

---

*This surface must be a cylindrical surface with generator parallel to the forward motion of the hydrofoil.

deriving Equation (2), it is assumed that the elastic forces are conservative and are proportional to the displacement amplitudes; and that generalized coordinates have been chosen such as to make the elastic coupling forces vanish. The generalized masses are obtained from $f_j(x,y)$ and the mass distribution per unit area $m(x,y)$ through the relation

$$M_{j\ell} = \iint m(x,y) \, f_\ell(x,y) \, f_j(x,y) \, dxdy \tag{3}$$

where the range of integration extends over all masses which participate in the motion.

The generalized forces in this study are restricted to those conservative forces which arise from the unsteady hydrodynamic pressure distribution $\Delta p(x,y,t)$. They are obtained from the relation

$$Q_j(t) = \iint \Delta p(x,y,t) \, f_j(x,y) \, dxdy \tag{4}$$

where the range of integration extends over the hydrofoil planform area.

Many hydrofoil structures can be considered as rigid in the chordwise direction, and the mode shapes $f_j(x,y)$ therefore divisible into r translational modes with spanwise distribution $[g_j(y) \; ; \; j = 1, \ldots, r]$, plus $n-r$ rotational modes with distribution $[g_j(y) \; ; \; j = r + 1, \ldots, n]$. Then Equation (1) becomes

$$z(x,y)T(t) = \sum_{j=1}^{r} g_j(y)q_j(t) + (eb-x) \sum_{j=r+1}^{n} g_j(y)q_j(t) \tag{5}$$

where b is the local semichord length and eb is the distance from the y-axis to the rotational axis of each section. Then, the generalized masses (3) can be written in terms of g_j , as can the spanwise distributions of mass $m(y)$, center of gravity $b(y) \, x_\alpha(y)$, and radius of gyration

4

$b(y) \, r_\alpha(y)$, which in turn are given by

$$m(y) \; = \; \int m(x,y) \; dx$$

$$bx_\alpha m(y) \; = \; \int (x-eb) m(x,y) \; dx$$

$$b^2 r_\alpha^2 m(y) \; = \; \int (x-eb)^2 \, m(x,y) \; dx$$

With these definitions, the generalized masses (3) become

$$M_{j\ell} = \begin{cases} \displaystyle\int m(y) g_\ell(y) g_j(y) \; dy & \begin{cases} j = 1, \, \ldots, \, r \\ \ell = 1, \, \ldots, \, r \end{cases} \\[3em] -\displaystyle\int bx_\alpha m(y) g_\ell(y) g_j(y) \; dy & \begin{cases} j = 1, \, \ldots, \, r \\ \ell = r+1, \, \ldots, \, n \end{cases} \\[3em] \displaystyle\int b^2 r_\alpha^2 m(y) g_\ell(y) g_j(y) \; dy & \begin{cases} j = r+1, \, \ldots, \, n \\ \ell = r+1, \, \ldots, \, n \end{cases} \\[3em] -\displaystyle\int bx_\alpha m(y) g_\ell(y) g_j(y) \; dy & \begin{cases} j = r+1, \, \ldots, \, n \\ \ell = 1, \, \ldots, \, r \end{cases} \end{cases} \qquad (6)$$

Then the generalized forces are brought to the form

$$Q_j(t) = \begin{cases} \displaystyle\int F(y,t) g_j(y) \; dy & ; & j = 1, \, \ldots, \, r \\[2em] \displaystyle\int T(y,t) g_j(y) \; dy & ; & j = r+1, \, \ldots, \, n \end{cases} \qquad (7)$$

where F and T are the lift and moment distribution per unit span

5

defined by

$$F(y,t) = \int \Delta p(x,y,t) \, dx$$

$$T(y,t) = \int (eb-x)\Delta p(x,y,t) \, dx$$

(8)

FLUTTER SPEED

When operating at the critical flutter speed (neutral oscillatory-dynamic stability), the motion of the hydrofoil will be harmonic. When one presumes that this condition has been attained, the equations of motion lead to a relation between the various parameters of the system which must be fulfilled during the flutter motion; and thus the critical flutter-speed boundary can be determined.

Therefore, harmonic motion is introduced in the form

$$q_j(t) = \bar{q}_j(\omega) \, e^{i\omega t} \quad ; \quad j = 1, \ldots, r$$

(9)

where $\bar{q}_j(\omega)$ is the complex amplitude of motion in the jth mode of displacement. When this motion has persisted for a sufficient length of time, its effects will also be harmonic with the same frequency ω ; then Q_j , Δp , F , and T can be written in the same form as $q_j(t)$ in Equation (9), and a common factor of $e^{i\omega t}$ can be cancelled from all equations. In particular, the displacement (5) becomes

$$Z(x,y) = \sum_{j=1}^{r} g_j(y)\bar{q}_j(\omega) + \sum_{j=r+1}^{n} (eb-x)g_j(y) \, \bar{q}_j(\omega)$$

(10)

and the equations of motion (2) can be written as

$$\omega^2 \sum_{\ell=1}^{n} \left[\left(\frac{\omega_\ell}{\omega} \right)^2 \delta_{j\ell} - 1 \right] M_{j\ell}\bar{q}_\ell(\omega) = \bar{Q}_j(\omega) \quad ; \quad j = 1,2, \ldots, n$$

(11)

6

where $\delta_{j\ell}$ represents the Kronecker delta defined by

$$\delta_{j\ell} = \begin{cases} 0 & ; \quad j \neq \ell \\ 1 & ; \quad j = \ell \end{cases}$$

and where the generalized forces are now given by

$$\overline{Q}_j(\omega) = \begin{cases} \int \overline{F}(y,\omega) g_j(y) \, dy & ; \quad j = 1, \ldots, r \\ \int \overline{T}(y,\omega) g_j(y) \, dy & ; \quad j = r+1, \ldots, n \end{cases} \tag{12}$$

$$\left. \begin{aligned} \overline{F}(y,\omega) &= \int \Delta\overline{p}(x,y,\omega) \, dx \\ \overline{T}(y,\omega) &= \int (eb-x)\Delta\overline{p}(x,y,\omega) \, dx \end{aligned} \right\} \tag{13}$$

In order to solve the equations of motion (11) for the unknown flutter speed and frequency, the harmonic force and moment per unit span (13) must be expressed in terms of the displacement (10). If the span of the hydrofoil is large and if the mode shapes, rotational axis location, and planform geometry change slowly in the spanwise direction, then the hydrodynamic force and moment per unit span can be closely approximated by that of two-dimensional hydrofoil sections with the same properties at each spanwise station. The unsteady lift in two-dimensional flow on a foil oscillating in heave $\overline{h}$ and pitch $\overline{\alpha}$ is given by

$$\overline{L}(y,\omega) = \pi\rho b^3 \omega^2 \left\{ L_h \frac{\overline{h}}{b} - \left[L_\alpha - (\tfrac{1}{2} + a) L_h \right] \overline{\alpha} \right\}$$

$$\overline{M}(y,\omega) = \pi\rho b^4 \omega^2 \left\{ -\left[M_h - (\tfrac{1}{2} + a) L_h \right] \frac{\overline{h}}{b} + \left[M_\alpha - (\tfrac{1}{2} + a)(M_h + L_\alpha) \right. \right.$$

$$\left. \left. + (\tfrac{1}{2} + a)^2 L_h \right] \overline{\alpha} \right\}$$

$$\tag{14}$$

7

where ab is the distance from the midchord to the rotational axis, positive aft, and where the lift and moment derivatives L_h , L_α , M_h , and M_α are expressed in terms of the Theodorsen function $C(k)$, by

$$L_h = 1 - \frac{2i}{k} C(k)$$

$$L_\alpha = \frac{1}{2} - \frac{2}{k^2} C(k) - \frac{i}{k} [1 + 2C(k)]$$

$$M_h = \frac{1}{2}$$ \hspace{3cm} (15)

$$M_\alpha = \frac{3}{8} - \frac{i}{k}$$

where $k = \omega b/U$ is the reduced frequency. The Theodorsen function can be evaluated by means of the relation

$$C(k) = F(k) + iG(k)$$ \hspace{2cm} (15a)

where

$$F(k) = \frac{J_1(k)\left[J_1(k) + Y_0(k)\right] - Y_1(k)\left[J_0(k) - Y_1(k)\right]}{\left[J_1(k) + Y_0(k)\right]^2 + \left[J_0(k) - Y_1(k)\right]^2}$$

$$G(k) = -\frac{J_0(k)J_1(k) + Y_0(k)Y_1(k)}{\left[J_1(k) + Y_0(k)\right]^2 + \left[J_0(k) - Y_1(k)\right]^2}$$

where J_n and Y_n are the nth order Bessel functions of the first and second kind, respectively. With displacement given by Equation (10), the heave and pitch amplitudes at station y are given by

$$\frac{\bar{h}}{b} = \sum_{\ell=1}^{r} g_\ell(y) \, \bar{q}_\ell(\omega)/b$$

$$\bar{\alpha} = \sum_{\ell=r+1}^{n} g_\ell(y) \, \bar{q}_\ell(\omega)$$

so that the harmonic force and moment per unit span (13) become

$$\bar{F}(y,\omega) = \pi\rho b^3 \omega^2 \cos \Lambda \left\{ L_h \sum_{\ell=1}^{r} g_\ell(y) \, \bar{q}_\ell(\omega)/b \right.$$

$$\left. - \left[L_\alpha - \left(\tfrac{1}{2} + a\right) L_h \right] \sum_{\ell=r+1}^{n} g_\ell(y) \, \bar{q}_\ell(\omega) \right\}$$

$$(16)$$

$$\bar{T}(y,\omega) = \pi\rho b^4 \omega^2 \cos \Lambda \left\{ -\left[M_h - \left(\tfrac{1}{2} + a\right) L_h \right] \sum_{\ell=1}^{r} g_\ell(y) \, \bar{q}_\ell(\omega)/b \right.$$

$$\left. + \left[M_\alpha - \left(\tfrac{1}{2} + a\right)(M_h + L_\alpha) + \left(\tfrac{1}{2} + a\right)^2 L_h \right] \sum_{\ell=r+1}^{n} g_\ell(y) \, \bar{q}_\ell(\omega) \right\}$$

where Λ is the midchord sweep angle. Combining Equations (12) and (16) yields

$$\bar{Q}_j(\omega) = \pi\rho\omega^2 \cos \Lambda \left\{ \sum_{\ell=1}^{r} \bar{q}_\ell(\omega) \int b^2 L_h \, g_\ell(y) g_j(y) \, dy \right.$$

$$\left. - \sum_{\ell=r+1}^{n} \bar{q}_\ell(\omega) \int b^3 \left[L_\alpha - \left(\tfrac{1}{2} + a\right) L_h \right] g_\ell(y) g_j(y) \, dy \right\} \; ;$$

$$j = 1, \ldots, r$$

$$(17)$$

$$\bar{Q}_j(\omega) = \pi\rho\omega^2 \cos \Lambda \left\{ - \sum_{\ell=1}^{r} \bar{q}_\ell(\omega) \int b^3 \left[M_h - \left(\tfrac{1}{2} + a\right) L_h \right] g_\ell(y) g_j(y) \, dy \right.$$

$$\left. + \sum_{\ell=r+1}^{n} \bar{q}_\ell(\omega) \int b^4 \left[M_\alpha - \left(\tfrac{1}{2} + a\right)(M_h + L_\alpha) + \left(\tfrac{1}{2} + a\right)^2 L_h \right] g_\ell(y) g_j(y) \, dy \right\} \; ;$$

$$j = r+1, \ldots, n$$

9

by which the generalized forces are related to the generalized coordinates $\bar{q}_j(\omega)$. Substituting Equations (17) into Equations (11), then dividing the translational equations $(j = 1, \ldots, r)$ by $\pi \rho \, b_0^3 \, \omega^2 s$, and the rotational equations $(j = r+1, \ldots, n)$ by $\pi \rho \, b_0^4 \, \omega^2 s$, where b_0 and s are suitable reference lengths in the chordwise and spanwise directions, yields the linear set of dimensionless homogeneous equations.

$$\sum_{\ell=1}^{r} \frac{\bar{q}_\ell(\omega)}{b_0} \left\{ \left[1 - \left(\frac{\omega_\ell}{\omega}\right)^2 \delta_{\ell j} \right] \frac{M_{\ell j}}{\pi \rho b_0^2 s} + \cos \Lambda \int_0^1 \left(\frac{b}{b_0}\right)^2 L_h \, g_\ell(y) g_j(y) \, dy \right\}$$

$$+ \sum_{\ell=r+1}^{n} \bar{q}_\ell(\omega) \left\{ \frac{M_{\ell j}}{\pi \rho b_0^3 s} - \cos \Lambda \int_0^1 \left(\frac{b}{b_0}\right)^3 \left[L_\alpha - (\tfrac{1}{2} + a) L_h \right] g_\ell(y) g_j(y) \, dy \right\} = 0 ;$$

$$j = 1, \ldots, r \qquad (18)$$

$$\sum_{\ell=1}^{r} \frac{\bar{q}_\ell(\omega)}{b_0} \left\{ \frac{M_{\ell j}}{\pi \rho b_0^3 s} - \cos \Lambda \int_0^1 \left(\frac{b}{b_0}\right)^3 \left[M_h - (\tfrac{1}{2} + a) L_h \right] g_\ell(y) g_j(y) \, dy \right\}$$

$$+ \sum_{\ell=r+1}^{n} \bar{q}_\ell(\omega) \left\{ \left[1 - \left(\frac{\omega_\ell}{\omega}\right)^2 \delta_{\ell j} \right] \frac{M_{\ell j}}{\pi \rho b_0^4 s} + \cos \Lambda \int_0^1 \left(\frac{b}{b_0}\right)^4 \right.$$

$$\left. \cdot \left[M_\alpha - (\tfrac{1}{2} + a)(M_h + L_\alpha) + (\tfrac{1}{2} + a)^2 L_h \right] g_\ell(y) g_j(y) \, dy \right\} = 0 ;$$

$$j = r+1, \ldots, n \qquad (19)$$

For these equations to have a non-trivial solution, the determinant of the coefficients of $\bar{q}_j$ is required to vanish; this yields the "flutter determinant." The values of speed (which appear in the reduced frequency) and of unknown frequency which make this determinant vanish are the predicted flutter speed U_f and flutter frequency ω_f.

The present study is concerned with the effect of sweep and taper on flutter speed. The planform geometry of the foils used in this study

Is shown in Figure 1. For a foil with midchord sweep angle Λ , the midchord-to-rotational-axis distance is given by

$$a = e(y) - \left[yA \tan \Lambda\right] / \frac{b}{b_0} \tag{20}$$

where $A = s/b_0$ with $b_0 = b(0) =$ root semichord length, and where s is the distance from root to tip in the direction normal to the flow. The semichord length is obtained from

$$\frac{b}{b_0} = 1 - (1-T) y \tag{21}$$

where $T = b(s)/b_0$, and the reduced frequency is obtained from

$$k = k_0 \frac{b}{b_0} \tag{22}$$

where

$$k_0 = \frac{\omega b_0}{U} \tag{23}$$

With these definitions, the relation between k_0 , ω , and the parameters of the system at the critical flutter speed is specified by the flutter determinant.

In the experimental part of the present study, the number of displacement modes was restricted to one in translation $(j = 1)$ and one in rotation $(j = 2)$, where the spanwise distribution of each mode was uniform; i.e.,

$$g_j(y) = 1 \quad ; \quad j = 1, \ldots, n \quad ; \quad n = 2 \tag{24}$$

The inertial terms in Equations (18) and (19) can be written in terms of the density ratio μ defined by

$$\mu = \frac{\int m(y) \, dy}{\pi \rho \, b_0^2 \, s} \tag{25}$$

11

Then, the dimensionless generalized masses are given by

$$\frac{M_{11}}{\pi\rho\, b_0{}^2\, s} = \mu$$

$$\frac{M_{12}}{\pi\rho\, b_0{}^3\, s} = \frac{M_{21}}{\pi\rho\, b_0{}^3\, s} = -\mu x_{\alpha_0} \qquad (26)$$

$$\frac{M_{22}}{\pi\rho\, b_0{}^4\, s} = \mu\, r_{\alpha_0}{}^2$$

where bx_α and $b^2 r_\alpha{}^2$ have been assumed constant along the span. The harmonic hydrodynamic derivatives are defined by

$$F_h = \cos\Lambda \int_0^1 \left(\frac{b}{b_0}\right)^2 L_h\, dy$$

$$F_\alpha = -\cos\Lambda \int_0^1 \left(\frac{b}{b_0}\right)^3 \left[L_\alpha - (\tfrac{1}{2} + a)\, L_h\right] dy$$

$$T_h = -\cos\Lambda \int_0^1 \left(\frac{b}{b_0}\right)^3 \left[M_h - (\tfrac{1}{2} + a)\, L_h\right] dy \qquad (27)$$

$$T_\alpha = \cos\Lambda \int_0^1 \left(\frac{b}{b_0}\right)^4 \left[M_\alpha - (\tfrac{1}{2} + a)(M_h + L_\alpha) + (\tfrac{1}{2} + a)^2\, L_h\right] dy$$

With these definitions, the flutter determinant obtained from Equations (18) and (19) reduces to the form

$$\begin{vmatrix} \mu\left[1 - \left(\dfrac{\omega_1}{\omega_2}\right)^2 \left(\dfrac{\omega_2}{\omega_f}\right)^2\right] + F_h & -\mu x_\alpha + F_\alpha \\[4mm] -\mu x_\alpha + T_h & \mu\, r_\alpha{}^2\left[1 - \left(\dfrac{\omega_2}{\omega_f}\right)^2\right] + T_\alpha \end{vmatrix} = 0$$

$$(28)$$

Since the hydrodynamic terms are complex, the expansion of the flutter determinant (28) yields a pair of simultaneous equations in the unknowns k_0 and ω_2/ω_f. An explicit solution of these equations cannot be obtained, due to the complicated dependence on k_0 which enters through Equations (15), (16), (22), and (27). On the other hand, if μ and ω_2/ω_f are considered the unknowns at specified values of k_0, then the imaginary part of the expansion of (28) leads to an equation of the form

$$\frac{1}{\mu} = \frac{A_i (\omega_2/\omega_f)^2 - B_i}{C_i} \tag{29}$$

where

$$A_i = (\omega_f/\omega_2)^2 \, T_{\alpha i} + r_\alpha^2 \, F_{hi}$$

$$B_i = T_{\alpha i} + r_\alpha^2 \, F_{hi} + x_\alpha (T_{hi} + F_{\alpha i}) \tag{30}$$

$$C_i = F_{hr} \, T_{\alpha i} + F_{hi} \, T_{\alpha r} - F_{\alpha r} \, T_{hi} - F_{\alpha i} \, T_{hr}$$

and where the real and imaginary parts of the harmonic hydrodynamic derivatives have been separated in the form

$$F_h = F_{hr} - \frac{i}{k_0} F_{hi}$$

$$F_\alpha = F_{\alpha r} + \frac{1}{k_0^2} F_{\alpha r}' - \frac{i}{k_0} F_{\alpha i}$$

$$T_h = T_{hr} - \frac{i}{k_0} T_{hi} \tag{31}$$

$$T_\alpha = T_{\alpha r} + \frac{1}{k_0^2} T_{\alpha r}' - \frac{i}{k_0} T_{\alpha i}$$

Combining Equations (15) and (27) yields relations for these quantities $(F_{hr}, \ldots, T_{\alpha i})$ directly in terms of $C(k)$. These are listed in the

Appendix. The function $C(k)$ can be evaluated by means of Equation (15a), with k given by Equation (22); hence these quantities can be evaluated easily with a suitable quadrature formula. (Simpson's Rule with twenty-one ordinates was used in this investigation.)

After elimination of μ by use of Equation (29), the real part of the expansion of (28) leads to an equation of the form

$$(\omega_2/\omega_f)^4 \, P - (\omega_2/\omega_f)^2 \, Q + R = 0 \tag{32}$$

where

$$P = D_r A_i^2/C_i^2 - E_r A_i/C_i + r_\alpha^2 (\omega_1/\omega_2)^2$$

$$Q = 2D_r A_i B_i/C_i^2 - E_r B_i/C_i - F_r A_i/C_i + r_\alpha^2 [1 + (\omega_1/\omega_2)^2]$$

$$R = D_r B_i^2/C_i^2 - F_r B_i/C_i + r_\alpha^2 - x_\alpha^2$$

$$A_r = (\omega_1/\omega_2)^2 \, T_{\alpha r} + r_\omega^2 F_{hr}$$

$$B_r = T_{\alpha r} + r_\alpha^2 F_{hr} + x_\alpha (F_{\alpha r} + T_{hr})$$

$$C_r = F_{hr} T_{\alpha r}' - F_{hi} T_{\alpha i} - F_{\alpha r}' T_{hr} + F_{\alpha i} T_{hi}$$

$$D_r = F_{hr} T_{\alpha r} - F_{\alpha r} T_{hr} + C_r/k_0^2$$

$$E_r = A_r + (\omega_1/\omega_2)^2 \, T_{\alpha r}'/k_0^2$$

14

$$F_r = B_r + (T_{\alpha r}' + x_\alpha F_{\alpha r}')/ k_0^2 \tag{33}$$

The roots of the quadratic Equation (32) can now be found, together with the values of μ from Equation (29). These roots determine the flutter frequency; the flutter speed is found from the relation

$$\frac{U_f}{b_0 \omega_2} = \frac{1}{k_0 (\omega_2/\omega_f)} \tag{34}$$

The solution of Equation (28) by means of this procedure has been carried out for the hydrofoil configurations used in the experimental part of this investigation.

QUASI-STEADY ANALYSIS

In earlier flutter analyses,[1-7] an asymptotic behavior of flutter speed has been found for density ratios, μ , in the range of practical interest for hydrofoils. The value of μ at which this asymptote occurs is known as the critical density ratio, μ_{CR} . Along this branch of the flutter-speed curve, one finds that $k_0 \to 0$ as $U_F \to \infty$. As a result, μ_{CR} can be predicted by using the quasi-steady approximation of the circulatory components of the lift plus the added mass.[*] The quasi-steady approximation is introduced by replacing $C(k)$ with a real constant F

---

[*] If the added mass were neglected as well, i.e., $k_0 = 0$, then the expansion of the flutter determinant would yield an expression for the divergence speed.

In Equations (15), which gives

$$L_h = 1 - \frac{2i}{k} F$$

$$L_\alpha = \tfrac{1}{2} - \frac{2}{k^2} F - \frac{i}{k} (1 + 2F)$$

$$M_h = \tfrac{1}{2}$$

$$M_\alpha = \tfrac{3}{8} - \frac{i}{k}$$

(35)

The dependence of the quasi-steady harmonic hydrodynamic derivatives on k_o is now given explicitly by Equations (31), where the quantities F_{hr} , ..., $T_{\alpha i}$ depend only on F and the foil geometry, and can be obtained from the expressions given in the Appendix with $G(k) = 0$ and $F(k) = F$.

Equation (28) can be expanded and solved for quasi-steady flutter speed and quasi-steady flutter frequency, as well as critical density ratio, in the form

$$\left(\frac{U_f}{b_o \omega_2} \right)^2 = \frac{\mu (A_2 \mu^2 + A_1 \mu + A_0)}{A_3 (\mu B_i + C_i)(\mu - \mu_{CR})}$$

(36)

where

$$A_0 = r_\alpha^2 (\omega_1/\omega_2)^2 C_i^2 - A_r A_i C_i + (F_{hr} T_{\alpha r} - F_{\alpha r} T_{hr}) A_i^2$$

$$A_1 = 2r_\alpha^2 (\omega_1/\omega_2)^2 B_i C_i - r_\alpha^2 [1 + (\omega_1/\omega_2)^2] A_i C_i - A_r A_i B_i + B_r A_i^2$$

$$A_2 = r_\alpha^2 (\omega_1/\omega_2)^2 B_i^2 - r_\alpha^2 [1 + (\omega_1/\omega_2)^2] A_i B_i + (r_\alpha^2 - x_\alpha^2) A_i^2$$

$$A_3 = (\omega_1/\omega_2)^2 B_i T_{\alpha r}' - A_i (T_{\alpha r}' + x_\alpha F_{\alpha r}')$$

$$\left(\frac{\omega_2}{\omega_f}\right)^2 = \frac{\mu\ B_i + C_i}{\mu\ A_i} \tag{37}$$

$$\mu_{CR} = \frac{A_1 C_r - C_i(\omega_1/\omega_2)^2 T_{\alpha r}'}{A_3} \tag{38}$$

For the case of a straight rectangular planform with $\omega_1/\omega_2 = 0$ the critical density ratio reduces to

$$\mu_{CR} = \frac{1}{1 + 2(x_\alpha + a)} \tag{39}$$

which is in agreement with the results presented by Henry, Henry and Ali, and Henry, Dugundji and Ashley.[1,2,14] The critical density ratio was predicted by means of Equation (38) for the hydrofoil configurations used in the experimental part of this investigation.

TRANSIENT RESPONSE

All results obtained from the equations of motion (18) and (19) — or, Equation (28) — are limited to the case of harmonic motion, since this condition is specified in the statement of the problem. (See Equation [9].) The results can be extended to more general motions by application of Fourier transform techniques; however, the indicial aerodynamics approach yields identical results with less analytical effort.

It is assumed that two-dimensional strip theory applies, so that the lift and moment per unit span due to translational and rotational motions $h(y,t)$ and $\alpha(y,t)$, respectively, can be written in the form

$$L(y,t) = \pi\rho b^2 (-\ddot{h} + U\dot{\alpha} - ba\ddot{\alpha}) - 2\pi\rho Ub \int_{-\infty}^{t} \ddot{H}(y,t)\ \emptyset(t-\tau)\ d\tau \tag{40}$$

$$M(y,t) = -\pi\rho b^2 \left[ba\ddot{h} + Ub(\tfrac{1}{2} - a)\,\dot{\alpha} + b^2(1/8 + a^2)\,\ddot{\alpha} \right]$$

$$- 2\pi\rho U b^2(\tfrac{1}{2} + a) \int_{-\infty}^{t} \ddot{H}(\tau)\emptyset(t-\tau)\, d\tau \tag{40}$$

where

$$\ddot{H}(y,t) = \ddot{h} - U\dot{\alpha} - b(\tfrac{1}{2} - a)\,\ddot{\alpha}$$

and where $\emptyset(t)$ is the Wagner function which is given approximately by

$$\emptyset(t) = 1 - .165\, e^{-.0455\, Ut/b} - .335\, e^{-.3\, Ut/b} \tag{41}$$

With displacement given by Equation (5), $h(t)$ and $\alpha(t)$ become

$$\dot{h}(y,t) = \sum_{\ell=1}^{r} g_\ell(y)\, q_\ell(t)$$

$$\tag{42}$$

$$\alpha(y,t) = \sum_{\ell=r+1}^{n} g_\ell(y)\, q_\ell(t)$$

Combining Equations (40) and (42) yields the force and moment $F(y,t)$ and $T(y,t)$ per unit span which, when inserted in Equation (7), give the generalized forces in the form

$$\underline{j=1,\ \ldots,\ r}$$

$$Q_j(t) = \pi\rho U^2 b_0 s \left\{ -\sum_{\ell=1}^{r} \frac{b_0 \ddot{q}_\ell(t)}{U^2} \int_0^1 \left(\frac{b}{b_0}\right)^2 g_j(y) g_\ell(y)\, dy \right.$$

$$+ \sum_{\ell=r+1}^{n} \frac{b_0 \dot{q}_\ell(t)}{U} \int_0^1 \left(\frac{b}{b_0}\right)^2 g_j(y) g_\ell(y)\, dy$$

18

$$-\sum_{\ell=r+1}^{n} \frac{b_0^2 \ddot{q}_\ell(t)}{U^2} \int_0^1 \left(\frac{b}{b_0}\right)^3 a\, g_j(y) g_\ell(y)\, dy$$

$$-2\sum_{\ell=1}^{r} \int_{-\infty}^{Ut/b_0} \frac{b_0 \dot{q}_\ell(\tau)}{U^2} \varphi(t-\tau)\, d\frac{U\tau}{b_0} \int_0^1 \left(\frac{b}{b_0}\right) g_j(y) g_\ell(y)\, dy$$

$$+2\sum_{\ell=r+1}^{n} \int_{-\infty}^{Ut/b_0} \frac{b_0 \dot{q}_\ell(\tau)}{U} \varphi(t-\tau)\, d\frac{U\tau}{b_0} \int_0^1 \left(\frac{b}{b_0}\right) g_j(y) g_\ell(y)\, dy$$

$$+2\sum_{\ell=r+1}^{n} \int_{-\infty}^{Ut/b_0} \frac{b_0^2 \ddot{q}_\ell(\tau)}{U^2} \varphi(t-\tau)\, d\frac{U\tau}{b_0} \int_0^1 \left(\frac{b}{b_0}\right)^2 (\tfrac{1}{2} - a)\, g_j(y) g_\ell(y)\, dy \Bigg\} \cos \Lambda$$

$$(43)$$

$$\underline{j = r+1,\ \ldots,\ n}$$

$$Q_j(t) = \pi\rho U^2 b_0^2 s \left\{ -\sum_{\ell=1}^{r} \frac{b_0 \ddot{q}_\ell(t)}{U^2} \int_0^1 \left(\frac{b}{b_0}\right)^3 a\, g_j(\ell)\, g_\ell(y)\, dy \right.$$

$$-\sum_{\ell=r+1}^{n} \frac{b_0 \dot{q}_\ell(t)}{U} \int_0^1 \left(\frac{b}{b_0}\right)^3 (\tfrac{1}{2} - a)\, g_j(y)\, g_\ell(y)\, dy$$

$$-\sum_{\ell=r+1}^{n} \frac{b_0^2 \ddot{q}_\ell(t)}{U^2} \int_0^1 \left(\frac{b}{b_0}\right)^4 (\tfrac{1}{8} + a^2)\, g_j(y)\, g_\ell(y)\, dy$$

$$-2\sum_{\ell=1}^{r} \int_{-\infty}^{Ut/b_0} \frac{b_0 \ddot{q}_\ell(\tau)}{U^2} \varphi(t-\tau)\, d\frac{U\tau}{b_0} \int_0^1 \left(\frac{b}{b_0}\right)^2 (\tfrac{1}{2} + a)\, g_j(y) g_\ell(y)\, dy$$

$$+ 2 \sum_{\ell=r+1}^{n} \int_{-\infty}^{Ut/b_0} \frac{b_0 \dot{q}_\ell(\tau)}{U} \varphi(t-\tau) \, d \frac{U\tau}{b_0} \int_0^1 \left(\frac{b}{b_0}\right)^2 (\tfrac{1}{2} + a) \, g_j(y) g_\ell(y) \, dy$$

$$+ 2 \sum_{\ell=r+1}^{n} \int_{-\infty}^{Ut/b_0} \frac{b_0^2 \ddot{q}_\ell(\tau)}{U^2} \varphi(t-\tau) \, d \frac{U\tau}{b_0} \int_0^1 \left(\frac{b}{b_0}\right)^3 (\tfrac{1}{4} - a^2) \, g_j(y) g_\ell(y) \, dy \Bigg\} \cos \Lambda$$

$$(44)$$

The equations of motion (2) can now be written in dimensionless form by dividing equations $j = 1, \ldots, r$ by $\pi \rho \, b_0 \, U^2 s$ and equations $j = r+1, \ldots, n$ by $\pi \rho \, b_0^2 \, U^2 s$, giving

$$\sum_{\ell=1}^{r} \frac{M_{j\ell}}{\pi \rho b_0^3 s} \frac{b_0 \ddot{q}_\ell}{U^2} + \sum_{\ell=r+1}^{n} \frac{M_{j\ell}}{\pi \rho b_0^3 s} \frac{b_0^2 \ddot{q}_\ell}{U^2} + \left(\frac{b_0 \omega_j}{U}\right)^2 \frac{M_{jj}}{\pi \rho b_0^2 s} \frac{q_j}{b_0} = \frac{Q_j}{\pi \rho b_0 U^2 s} ;$$

$$j = 1, \ldots, r \qquad (45)$$

$$\sum_{\ell=1}^{r} \frac{M_{j\ell}}{\pi \rho b_0^3 s} \frac{b_0 \ddot{q}_\ell}{U^2} + \sum_{\ell=r+1}^{n} \frac{M_{j\ell}}{\pi \rho b_0^4 s} \frac{b_0^2 \ddot{q}_\ell}{U^2} + \left(\frac{b_0 \omega_j}{U}\right)^2 \frac{M_{jj}}{\pi \rho b_0^4 s} q_j = \frac{Q_j}{\pi \rho b_0^2 U^2 s} ;$$

$$j = r+1, \ldots, n \qquad (46)$$

The solution of these equations of motion (45) and (46), together with the generalized forces given by Equations (43) and (44), can be found by Laplace transform methods. This procedure has been carried out for the two-degree-of-freedom hydrofoil models which were used in the experimental part of this investigation. For this case,

$$r = 1 \qquad ; \qquad n = 2$$

$$g_j(y) = 1 \qquad ; \qquad j = 1,2$$

20

and the equations of motion reduce to

$$\mu \ddot{q}_1{}^* - \mu x_\alpha \ddot{q}_2{}^* + \Omega_1{}^2 \mu q_1{}^* = Q_1{}^*(t^*) \left. \vphantom{\int} \right\}$$

$$- \mu x_\alpha \ddot{q}_1{}^* + \mu r_\alpha{}^2 \ddot{q}_2{}^* + \Omega_2{}^2 \mu r_\alpha{}^2 q_2{}^* = Q_2{}^*(t^*) \left. \vphantom{\int} \right\} \qquad (47)$$

where the "*" denotes the corresponding dimensionless quantities of Equations (45) and (46) and where

$$\Omega_j = \frac{\omega_j b_0}{U} \qquad (48)$$

Taking the Laplace transform of Equation (47) and introducing the initial conditions

$$\dot{q}_1{}^*(0) = q_2{}^*(0) = \dot{q}_2{}^*(0) = 0$$

$$q_1{}^*(0) = h_0$$

yields the algebraic equations

$$\bar{q}_1 \left\{ p^2 \left[\mu + \int_0^1 \left(\frac{b}{b_0}\right)^2 dy^* \right] + \mu \Omega_1{}^2 + 2p\bar{\varphi} \left[p \int_0^1 \left(\frac{b}{b_0}\right) dy^* \right] \right\}$$

$$+ \bar{q}_2 \left\{ p^2 \left[- \mu x_\alpha + \int_0^1 \left(\frac{b}{b_0}\right)^3 a \, dy^* \right] - p \int_0^1 \left(\frac{b}{b_0}\right)^2 dy^* - 2p\bar{\varphi} \right.$$

$$\left. \cdot \left[p \int_0^1 \left(\frac{b}{b_0}\right)^2 (\tfrac{1}{2} - a) \, dy^* + \int_0^1 \left(\frac{b}{b_0}\right) dy^* \right] \right\}$$

$$= h_0 \left\{ p \left[\mu + \int_0^1 \left(\frac{b}{b_0}\right)^2 dy^* \right] + 2p\bar{\varphi} \int_0^1 \left(\frac{b}{b_0}\right) dy^* \right\}$$

$$(49)$$

and

$$\bar{q}_1 \left\{ p^2 \left[-\mu x_\alpha + \int_0^1 \left(\frac{b}{b_0}\right)^3 a \, dy^* \right] + 2p\bar{\varphi} \left[p \int_0^1 \left(\frac{b}{b_0}\right)^2 \left(\tfrac{1}{2} + a\right) dy^* \right] \right\}$$

$$+ \bar{q}_2 \left\{ p^2 \left[\mu r_\alpha^2 + \int_0^1 \left(\frac{b}{b_0}\right)^4 \left(\tfrac{1}{8} + a^2\right) dy^* \right] + p \int_0^1 \left(\frac{b}{b_0}\right)^3 \left(\tfrac{1}{2} - a\right) dy^* + \mu r_\alpha^2 \Omega_2^2 \right.$$

$$\left. - 2p\bar{\varphi} \left[p \int_0^1 \left(\frac{b}{b_0}\right)^3 \left(\tfrac{1}{4} - a^2\right) dy^* + \int_0^1 \left(\frac{b}{b_0}\right)^2 \left(\tfrac{1}{2} + a\right) dy^* \right] \right\}$$

$$= h_0 \left\{ p \left[-\mu x_\alpha + \int_0^1 \left(\frac{b}{b_0}\right)^3 a \, dy^* \right] + 2p\bar{\varphi} \int_0^1 \left(\frac{b}{b_0}\right)^2 \left(\tfrac{1}{2} + a\right) dy^* \right\}$$

where $dy^* = \cos \Lambda \, dy$ (50)

where p is the Laplace transform variable, the bar indicates Laplace transformation, and

$$\bar{\varphi}(p) = \frac{1}{p} - \frac{.165}{p + .0455} - \frac{.335}{p + .3} \tag{51}$$

Expanding the determinant of the coefficients of $\bar{q}_1$ and $\bar{q}_2$ in Equations (49) and (50), then multiplying by $[(p + .0455)(p + .3)]^2$ in order to clear fractions, leads to an eighth-order polynomial in p. The real and imaginary parts of the roots of this polynomial are the decay rate σ and frequency ω of the transient response of the system. These calculations have been carried out for the cases of the hydrofoil models used in the experimental part of this study.

EXPERIMENTAL ANALYSIS

FLUTTER APPARATUS

The Davidson Laboratory Flutter Apparatus[1] was used in the experimental phase of this investigation. The flexure system described in Volume II of the series of reports relating to this study[2] was used to support the models, and the thicknesses of the flexures were adjusted to obtain the properties listed in Table I. The upper and lower end plates were retained to negate end effects.

MODELS

Four hydrofoil models were constructed, each with the NACA 0012 cross section, 6-in. chord and 12-in. span. Two of these models had midchord sweep angles of 15 degrees and 45 degrees, with no taper, while the remaining pair had taper ratios of 2/3 and 1/3 with a midchord sweep angle of zero degrees. During calibration, it was found that the mass of the model with sweep angle of 45 degrees could not be varied without significant changes in the radius of gyration and center-of-gravity location. Therefore, no flutter tests were conducted with this model. The properties of the remaining three models are summarized in Table 2.

CALIBRATIONS

The center-of-gravity weights and additional weights were designed and constructed following the procedure described in Volume I of this series of reports.[1] The uncoupled natural frequencies ω_1 and ω_2 in translation and rotation, respectively, were measured in air and the values are reported in Table 3 for those configurations used in the flutter tests. These values of the uncoupled natural frequencies are exhibited in Figure 2; their variation with respect to $1/\sqrt{\mu}$ is substantially linear, indicating

23

that the uncoupled natural-frequency ratio is nearly constant for all configurations. Furthermore, the radius of gyration r_α is related to the uncoupled natural-frequency ratio through the expression

$$r_\alpha{}^2 = \frac{1}{b_0{}^2} \frac{K_2}{K_1} \left(\frac{\omega_1}{\omega_2}\right)^2 \tag{40}$$

where K_1 and K_2 are the support stiffnesses in translation and rotation, respectively. Therefore, r_α is also nearly constant for all configurations.

TEST PROCEDURE AND DATA ANALYSIS

The response characteristics of each of the configurations described above was investigated over a range of speeds in DL Tank 3. The model was given an initial displacement and locked in position before each run. After the apparatus had reached a constant speed, the model was released and the time histories of the translational and rotational motions were recorded. The apparatus was then returned to the starting position and the water was allowed to settle for about five minutes before the next run. The speed was increased in each subsequent run, until a flutter condition was obtained or until the maximum speed of about 15 fps was reached.

The decay rate and frequency of response were obtained from the recorded motions by means of the procedure described in Volume I of this series of reports.[1] These results are presented in Table 4 and in Figures 3, 4, and 5, for the three models used in this investigation.

DISCUSSION OF RESULTS

Measured values of decay rate, frequency, and flutter speed are compared herein with the corresponding results predicted by two-dimensional airfoil theory applied in a stripwise manner. The dynamic configuration of the hydrofoil models includes only two degrees of freedom, viz., uniform translation and rotation about a spanwise axis. Three hydrofoil models are considered (with properties listed in Table 2), each supported with two degrees of freedom. Table 3 exhibits the elastic and inertial properties of the test configurations; and Table 4 shows the measured values of speed, frequency, and decay rate, in dimensionless form. Note that a negative decay rate indicates a stable response and vice versa.

The measured decay rate σ and frequency ω for Model 1 are shown in Figures 3a and 3b for the two density ratios, μ , tested. The corresponding theoretical results, predicted by the methods described in the previous section, are also shown (see Theoretical Analysis, Transient Response). The predicted response frequency is in agreement with the measured value, whereas the measured decay rate is not. In fact, at $\mu = 3.43$ in Figure 3b, the experimental results indicate a critical flutter speed at $U_f/b_0\omega_2 = 2.4$, while the theory predicts stable response at all speeds.

The same comparison is made for Models 3 and 4 in Figures 4 and 5, respectively. Again agreement is found between measured and predicted frequencies, but the predicted decay rate is larger (more stable) than the measured one, near flutter.

The measured flutter speeds for Models 1, 2, and 3 are compared in Figures 6, 7, and 8, respectively, with values predicted by the flutter-analysis procedure described previously (see Theoretical Analysis, Flutter Speed). The non-conservative discrepancy described in Volumes I and II of this series of reports[1,2] and by Woolston and Castile[6] appears again in the present study where sweep and taper have been introduced. Since the dynamic configuration used in these tests is highly simplified, it is not evident

25

to what extent the conclusions reached here will apply to actual hydrofoil systems. However, since the present results and those of Volumes I and II show the theory to be non-conservative for the prediction of flutter speed and decay rate, it is suggested that in hydrofoil design studies the theory be used only as an indication of the proximity of an unstable condition. Model tests should be carried out when flutter appears imminent.

In order to show the effect of sweep angle for this configuration, the flutter speed was calculated over a range of sweep angle. The results, exhibited in Figure 9, show that the flutter speed increases with increasing sweep angle and that, furthermore, the critical density ratio increases (Figures 9 and 10). The results shown in Figure 10 were calculated by means of the quasi-steady analysis; in particular, by Equation (38).

The same calculations, carried out over a range of taper ratio, led to the results shown in Figures 11 and 12. The flutter speed may increase or decrease with increasing taper, depending on the range of density ratio. For $\mu < 1$, which is of interest for hydrofoil craft, increasing taper (decreasing taper ratio) leads to lower flutter speeds (Figure 11), as well as lower values of the critical density ratio (Figures 11 and 12). Thus, for this dynamic configuration, increasing sweep angle or decreasing taper yields higher flutter speeds and higher values of the critical density ratio.

It has been suggested by several investigators that a simplified, quasi-steady representation of the unsteady hydrodynamic forces can be used to predict the flutter speed of hydrofoils.[11,12] In order to provide evidence counter to this suggestion, the quasi-steady flutter speed was calculated by means of Equations (35) and (36) with $C(k) = F = 1.0$ and 0.5 . The results of this calculation for the case of the hydrofoil models tested in this study are shown in Figures 6, 7, and 8; also shown is the flutter speed predicted by using the exact $C(k)$. In addition, the same calculations are shown in Figures 13 through 16 for the models tested earlier.[1,2] No consistent agreement is found between the quasi-steady and unsteady results, nor is any consistent agreement shown between quasi-steady predictions and measured flutter speeds. Hence flutter speeds predicted by quasi-steady analyses are not reliable.

In a subsequent report, the comparison of measured and predicted flutter speeds for the two-degree-of-freedom system will be extended to models with rectangular planform and finite aspect ratio and to a model with sweep, taper, and finite aspect ratio. The measured flutter speeds will be compared with predictions based on lifting-surface theory and two-dimensional strip theory.

CONCLUSIONS

Measured and predicted values of the decay rates, frequencies, and flutter speeds of hydrofoils are compared herein for the case of a two-degree-of-freedom system. Three hydrofoil models are considered: one with a midchord sweep angle of 15 degrees and no taper, the others with taper ratios of 2/3 and 1/3 with no sweep. The tests were conducted over a range of speeds and density ratios.

It is shown that the non-conservative discrepancy between measured and predicted decay rates and flutter speeds, which was found in previous studies,[1,2] appears again in the present results where sweep and taper have been introduced. Thus, it is suggested that theoretical calculations be used only for an indication of the proximity of a flutter boundary, and that model tests be carried out when flutter appears imminent.

Calculated values of flutter speed based on two-dimensional strip theory for the two-degrees-of-freedom model show that increasing sweep angle or decreasing taper yields higher flutter speeds as well as higher values of critical density ratio.

No consistent agreement is found between the quasi-steady and unsteady predictions of flutter speed for the two-degree-of-freedom system, nor is any consistent agreement shown between quasi-steady predictions and measured flutter speeds. Hence, flutter speeds predicted by a quasi-steady analysis are not reliable.

27

REFERENCES

1. HENRY, C. J., "Hydrofoil Flutter Phenomenon and Airfoil Flutter Theory; Vol. I, Density Ratio," DL Report 856, September 1961.

2. HENRY, C. J. and ALI, M. R., "Hydrofoil Flutter Phenomenon and Airfoil Flutter Theory; Vol. II, Center of Gravity Location," DL Report 911, July 1962.

3. CHU, W. H. and ABRAMSON, H. N., "An Alternative Formulation of the Problem of Flutter in Real Fluids," Technical Report No.2, Contract Nonr 2470(00), SWRI Project 19-754-2, Southwest Research Institute, October 1959.

4. ROTT, N. and GEORGE, M. B. T., "An Approach to the Flutter Problem in Real Fluids," Preprint No. 509, Institute of Aeronautical Sciences, 1955.

5. JEWELL, D. A. and McCORMICK, M. E., "Hydroelastic Instability of a Control Surface," Journal of Ship Research, Vol. 6, No. 1, June 1962.

6. WOOLSTON, D. S. and CASTILE, G. E., "Some Effects in Variations in Several Parameters Including Fluid Density on the Flutter of Light Uniform Cantilever Wings," NACA TN 2558, 1951.

7. HENRY, C. J. and ALI, M. R., "Surface-piercing Hydrofoil Flutter," DL Report 992, November 1963.

8. TSAKONAS, S. and HENRY, C. J., "Three-Dimensional Gust Problem in the Presence of the Free Surface," DL Note 705, September 1963.

9. HENRY, C. J., "Indicial Three-Dimensional Lifting Surface Theory Near a Free Surface," Dissertation, Stevens Institute of Technology, June 1965.

10. HENRY, C. J. and ALI, M. R., "Hydroelastic Study of Elastic Beams with a Foil-Shaped Appendage," DL Report 1022, July 1964.

11. McGOLDRICK, R. T., "Rudder Excited Hull Vibrations on USS Forrest Sherman (DD 931) — A Problem in Hydroelasticity," Transactions SNAME, Vol. 67, 1959.

12. LEIBOWITZ, R. C. and BELZ, D. J., "Comparison of Theory and Experiment for Marine Control-Surface Flutter," Fourth Symposium on Naval Hydrodynamics, August 1962.

13. BISPLINGHOFF, R. L., ASHLEY, H., HALFMAN, R. L., <u>Aeroelasticity</u>,
    Addison-Wesley Publishing Co., Reading, Mass., 1955.

14. HENRY, C. J., DUGUNDJI, J., and ASHLEY, H., "Aeroelastic Stability of
    Lifting Surfaces in High Density Fluids," <u>Journal of Ship Research</u>
    Vol. 2, No. 4, March 1959.

TABLE 1

PROPERTIES OF DAVIDSON LABORATORY FLUTTER APPARATUS WITH NO WEIGHTS OR MODELS

(Reference span length, 12 in.; reference semichord length, 3 in.)

K_1 = 0.203 lb/in.^{2}

K_2 = 3.68 in.-lb/in.-rad $\qquad$ μ_o = 0.413

ω_1 = 13.3 rad/sec $\qquad$ $r_{\alpha_o}^2$ = 0.150

ω_2 = 48.7 rad/sec $\qquad$ x_{α_o} = 0.092

TABLE 2

PROPERTIES OF MODELS

Model	Description	μ_m	x_{α_m}	e_o
1	Span-chord ratio, 2 Sweep angle, 15° (no taper)	0.168	0.40	0.0
2	Span-chord ratio, 2 Taper ratio, 2/3 (no sweep)	0.204	0.280	-0.4
3	Span-chord ratio, 2 Taper ratio, 1/3 (no sweep)	0.143	0.285	-0.4

30

TABLE 3

MEASURED PROPERTIES OF TEST CONFIGURATION

Model	CG WEIGHTS Position ① (inches)	②	Weight [each] (lb)	x_α	μ	ω_2 rad/sec	ω_1/ω_2	r_α
1	-4.0	5.3	0.5	0.189	3.02	9.54	0.530	0.752
					3.43	8.94	0.530	0.752
2	-3.5	6.9	0.5	0.204	1.00	16.6	0.528	0.748
					1.14	15.7	0.526	0.746
					1.27	14.8	0.527	0.747
					1.81	12.2	0.534	0.757
					2.34	10.7	0.537	0.762
3	-3.4	6.6	0.5	0.194	0.94	17.4	0.520	0.738
					1.08	16.2	0.523	0.742
					1.74	12.4	0.535	0.758
					2.27	10.9	0.534	0.757
					2.83	10.06	0.518	0.734

TABLE 4

MEASURED RESPONSE CHARACTERISTICS

Model	μ	$U/b\omega_2$	ω/ω_2	σ/ω_2	$\omega b/U$
1	3.02	1.44	0.820	-0.194	0.568
		1.96	0.834	-0.086	0.426
		2.52	0.815	-0.022	0.324
		2.84	0.814	-0.009	0.286
		2.94	0.820	-0.008	0.279
	3.43	2.06	0.933	-0.071	0.452
		2.20	0.806	-0.049	0.367
		2.55	0.845	+0.027	0.331
2	0.987	2.49	0.868	-0.045	0.349
		2.79	0.855	-0.090	0.307
	1.00	1.46	0.898	-0.074	0.615
		1.88	0.893	-0.037	0.474
		2.10	0.91	-0.044	0.433
		2.40	0.882	-0.037	0.368
	1.140	1.42	0.898	-0.044	0.632
		1.53	0.888	-0.037	0.579
		1.60	0.888	-0.019	0.557
		1.70	0.885	-0.017	0.522
		1.80	0.876	-0.007	0.484
		2.02	0.88	+0.026	0.435
	1.27	1.10	0.902	-0.08	0.82
		1.35	0.885	-0.043	0.656
		1.63	0.887	-0.003	0.544
		1.68	0.892	+0.006	0.530

Mode	μ	$U/b\omega_a$	ω/ω_a	σ/ω_a	$\omega b/U$
2	1.81	0.99	0.952	-0.082	0.964
		1.16	0.917	-0.048	0.794
		1.28	0.898	-0.029	0.702
		1.40	0.882	+0.001	0.630
	2.34	0.97	0.952	-0.068	0.985
		1.28	0.909	-0.035	0.709
		1.39	0.896	-0.018	0.643
		1.64	0.878	+0.051	0.536
3	0.925	1.48	0.901	-0.074	0.611
		2.03	0.913	-0.038	0.451
	0.94	1.50	0.905	-0.027	0.604
		1.71	0.912	-0.022	0.532
		1.87	0.941	-0.017	0.504
		1.93	0.926	+0.02	0.480
	1.08	1.11	0.934	-0.072	0.838
		1.28	0.916	-0.051	0.714
		1.35	0.934	-0.025	0.689
		1.48	0.912	-0.039	0.617
		1.61	0.908	-0.003	0.562
		1.69	0.908	+0.015	0.539
	1.74	1.01	0.974	-0.053	0.962
		1.30	0.937	-0.020	0.719
		1.51	0.920	+0.019	0.611
		1.58	0.909	+0.030	0.576
	2.27	0.93	0.978	-0.063	1.048
		1.32	0.937	-0.023	0.709
		1.42	0.928	-0.010	0.654
		1.53	0.912	+0.019	0.598

Mode	μ	$U/b\omega_a$	ω/ω_a	σ/ω_a	$\omega b/U$
3	2.83	1.30	0.925	-0.036	0.713
		1.45	0.909	-0.019	0.626
		1.55	0.893	0.0	0.576
		1.60	0.882	+0.022	0.552
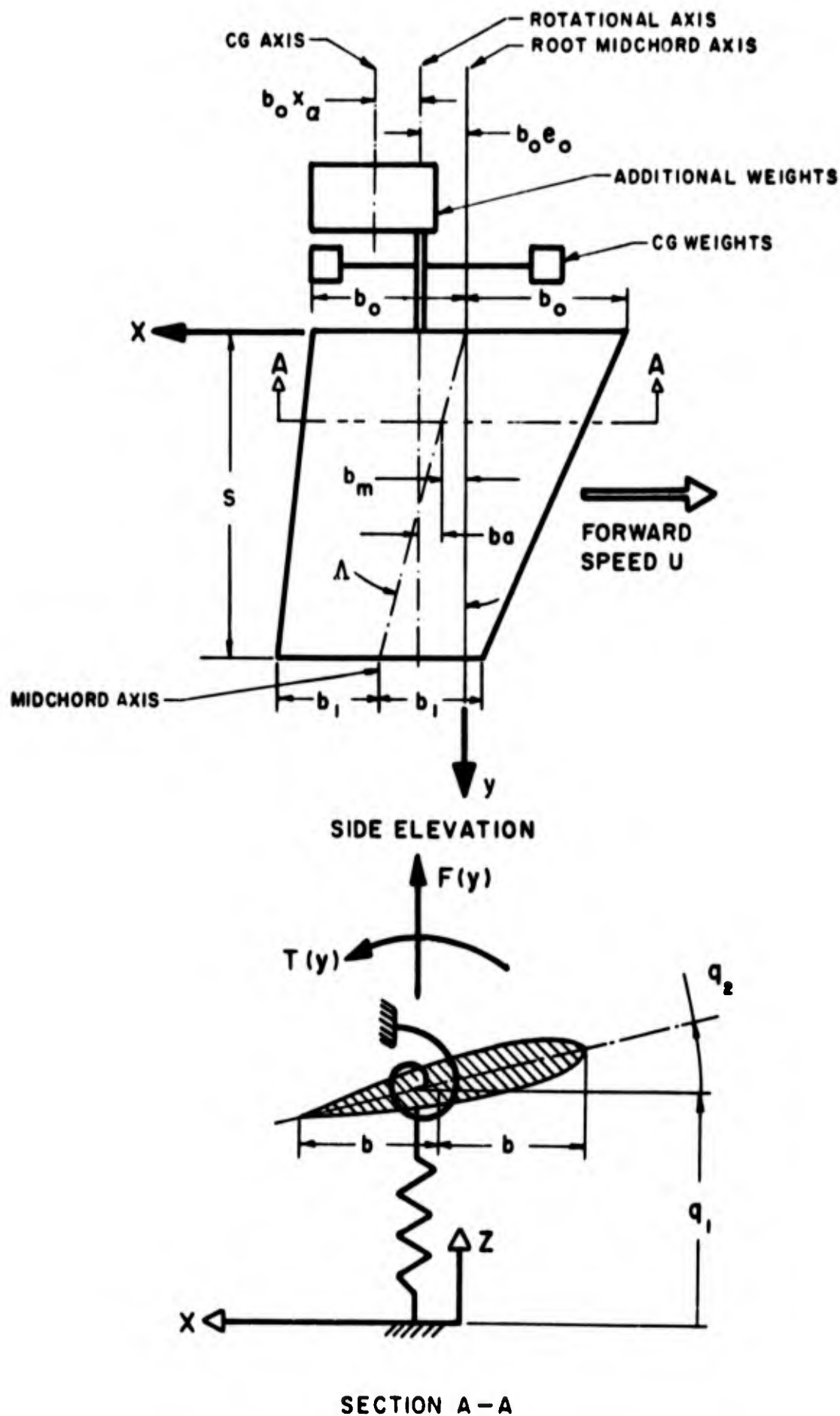
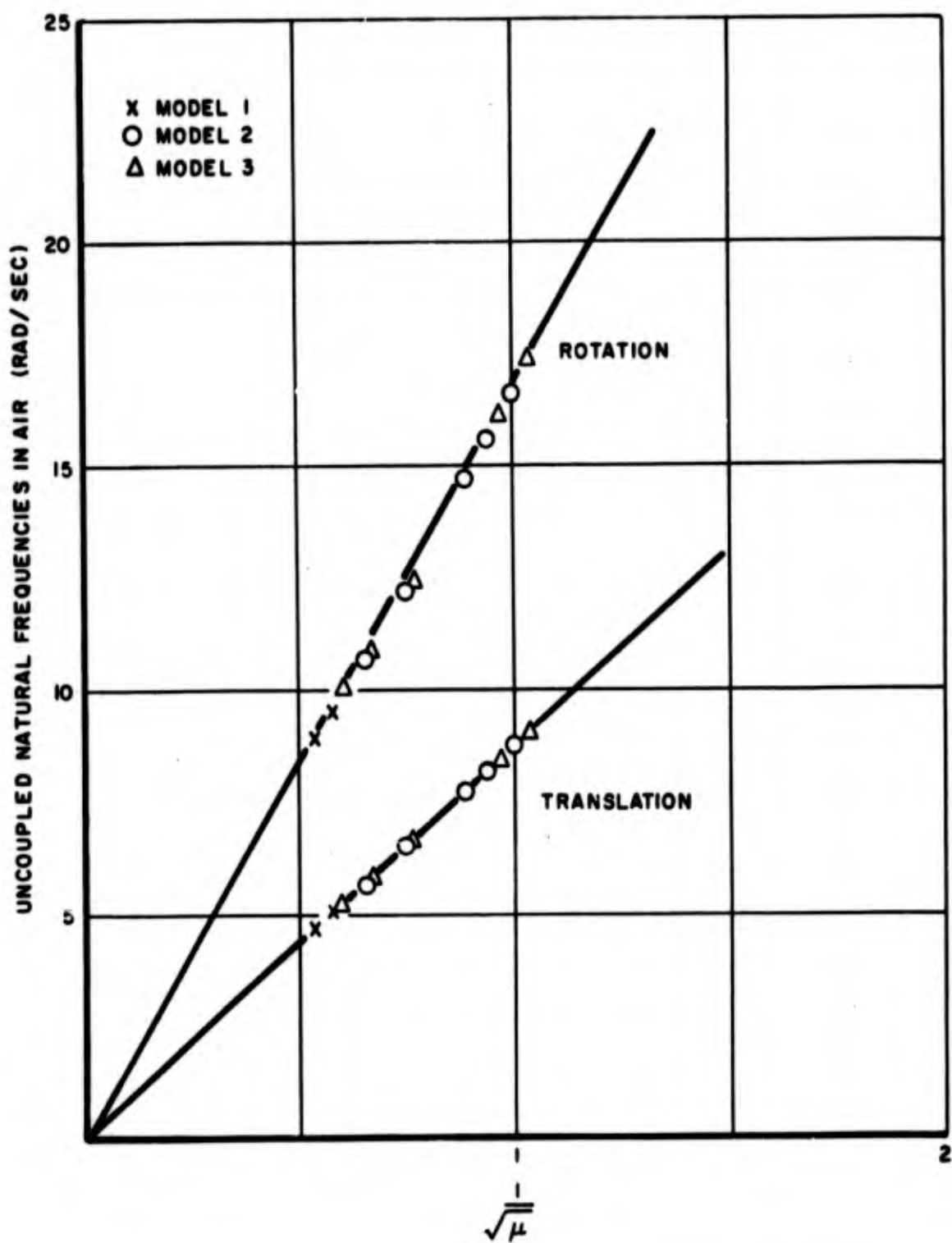**FIGURE 1. SCHEMATIC DIAGRAM OF HYDROFOIL MODEL WITH DEFINITION OF PARAMETERS AND COORDINATE SYSTEM**
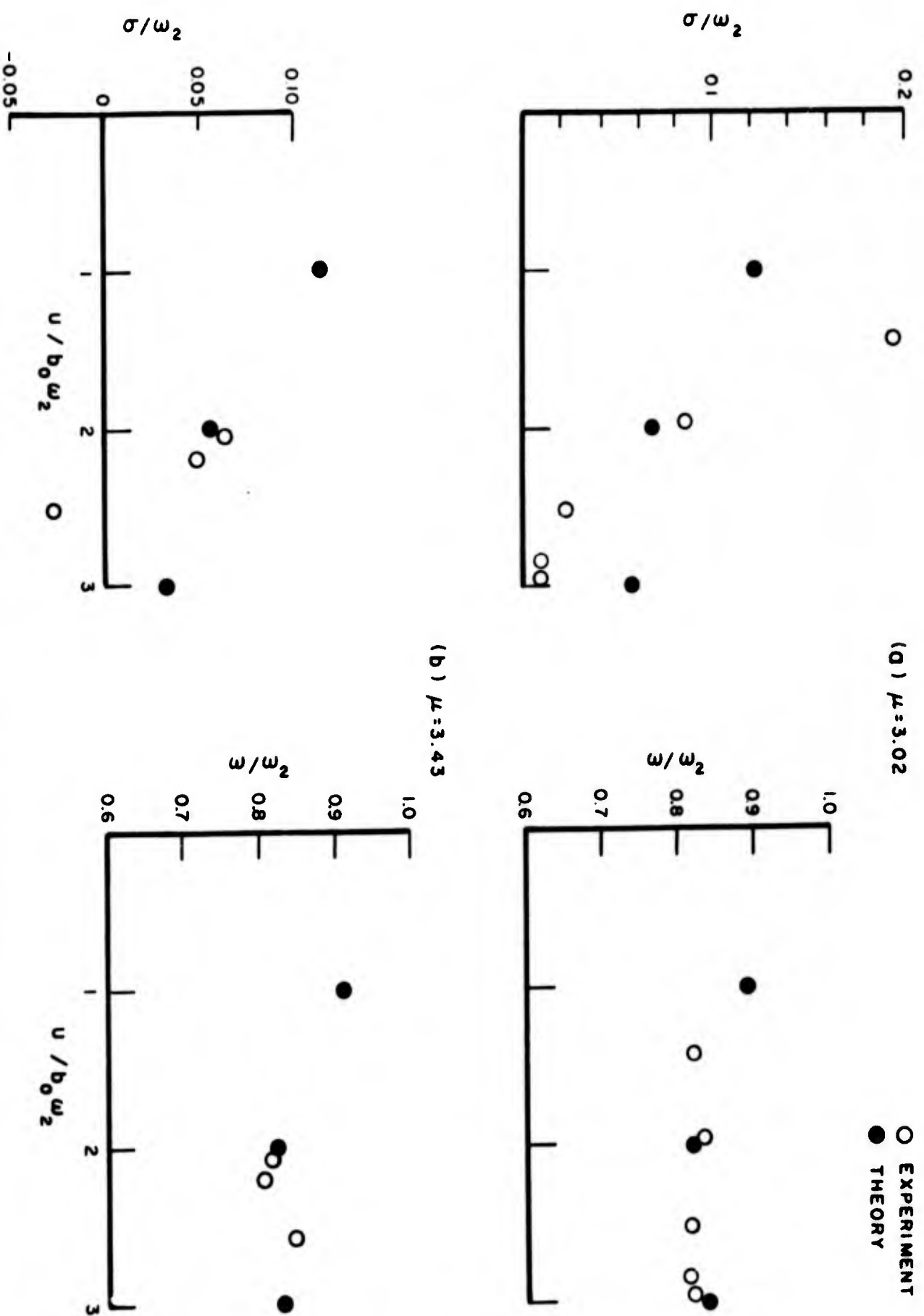
FIGURE 2.   UNCOUPLED NATURAL FREQUENCIES

FIGURE 3. RESPONSE CHARACTERISTICS — MODEL I
SWEEP ANGLE 15° — NO TAPER

R-1115
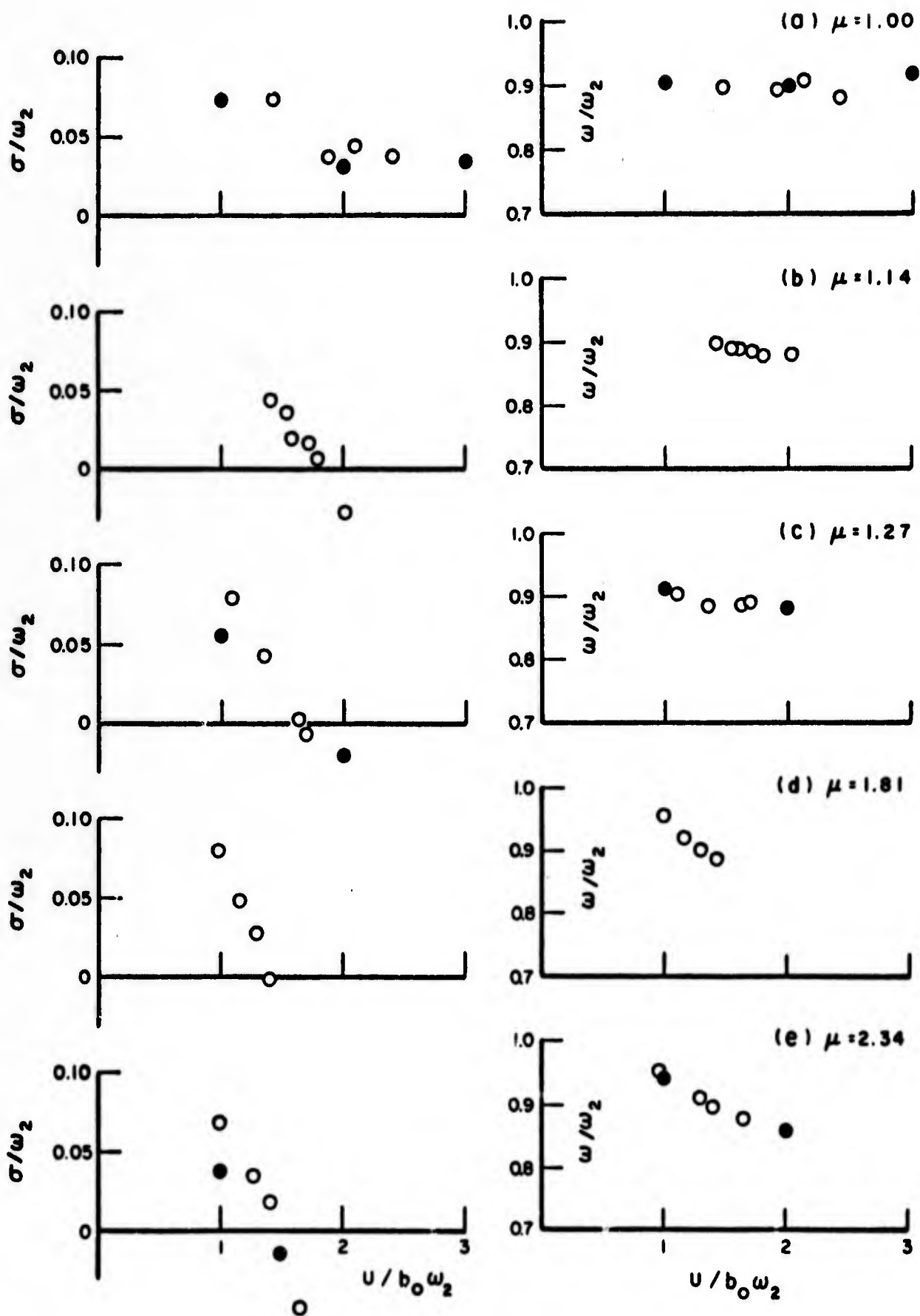
FIGURE 4. RESPONSE CHARACTERISTICS – MODEL 2
NO SWEEP TAPER RATIO 2/3
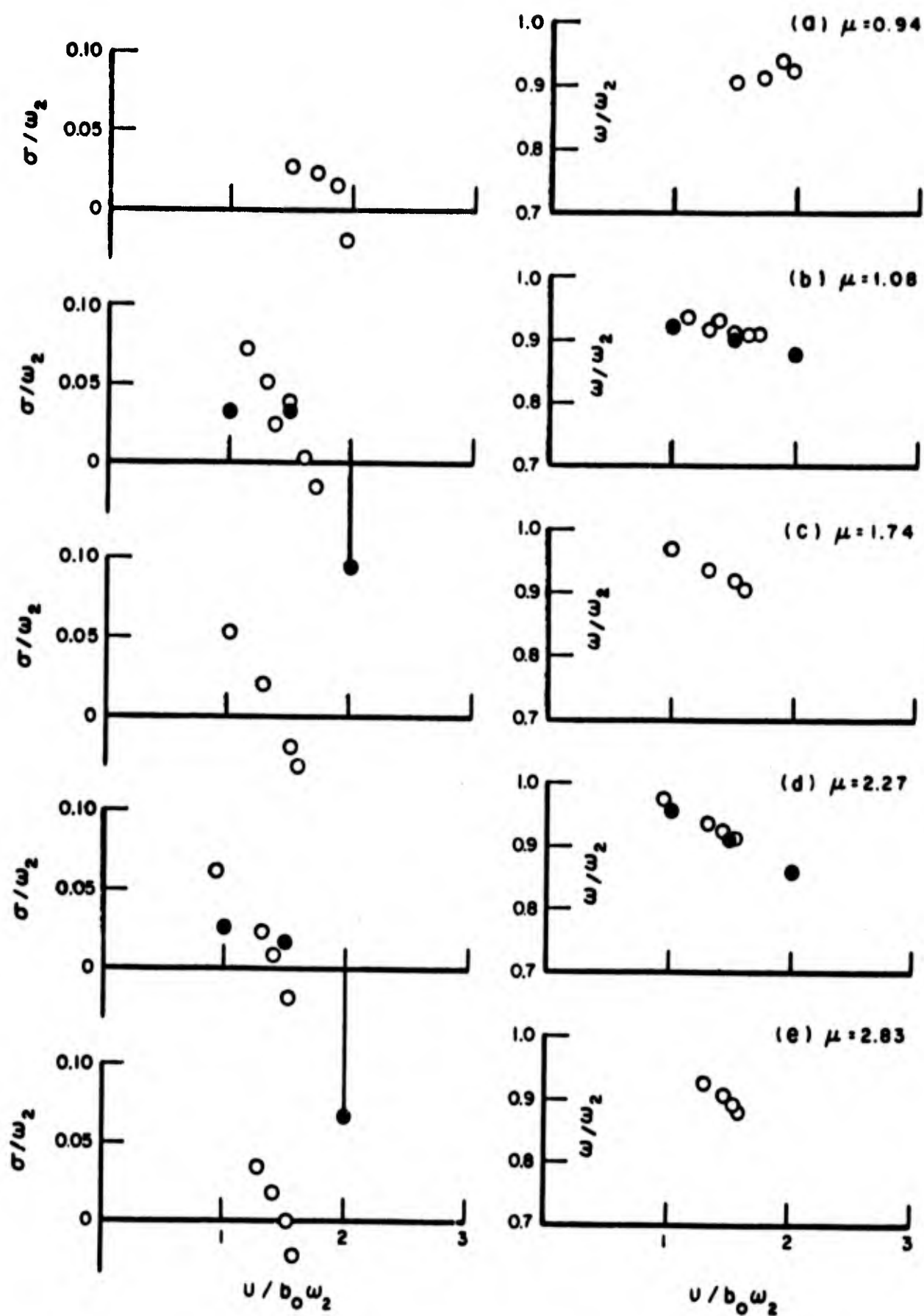
FIGURE 5.   RESPONSE CHARACTERISTICS — MODEL 3
NO SWEEP   TAPER RATIO 1/3

BLANK PAGE
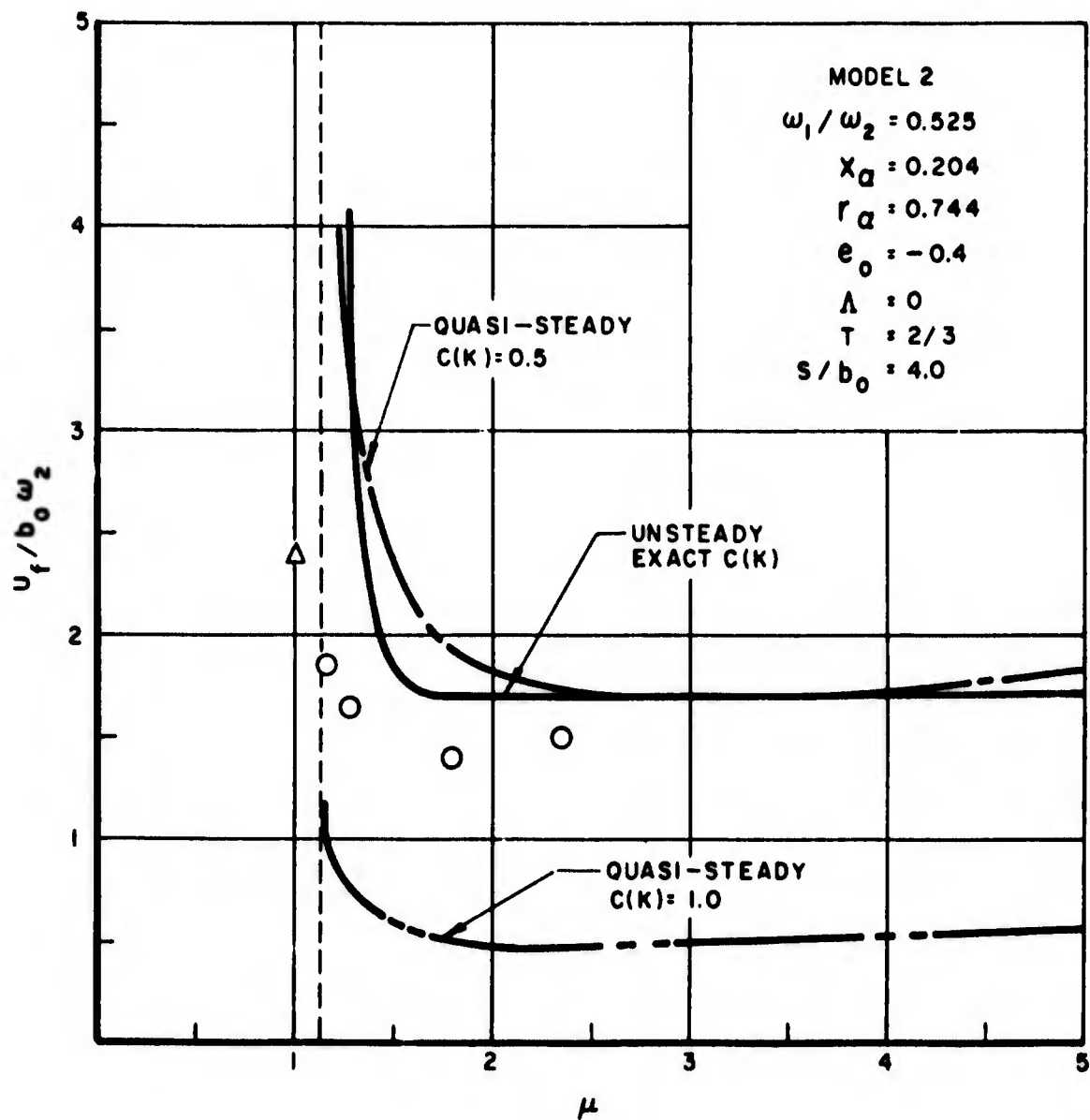
FIGURE 7. COMPARISON OF UNSTEADY, QUASI-STEADY AND
EXPERIMENTAL FLUTTER SPEEDS FOR A TWO-DEGREE-
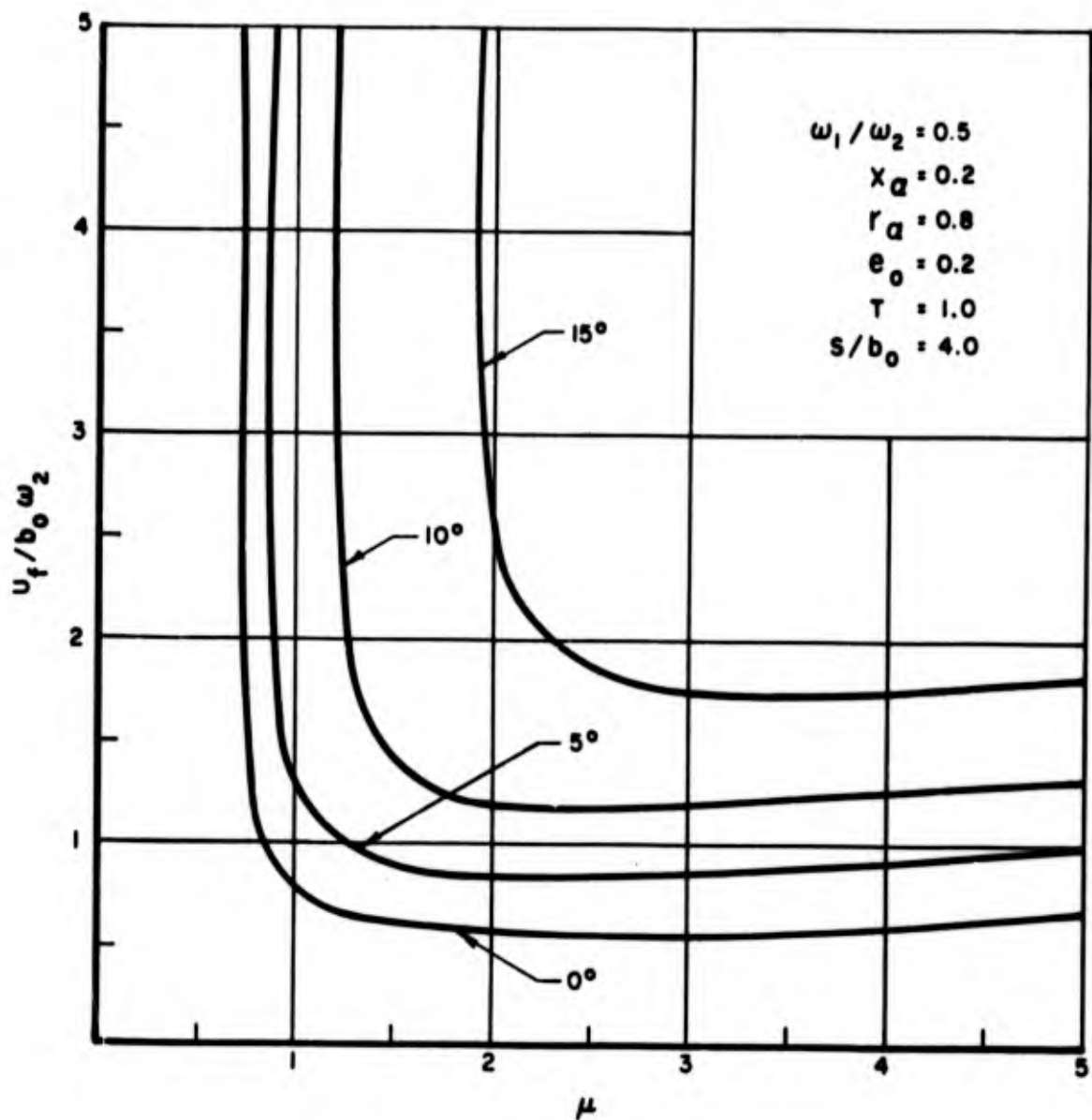OF-FREEDOM HYDROFOIL MODEL IN TWO DIMENSIONAL
FLOW
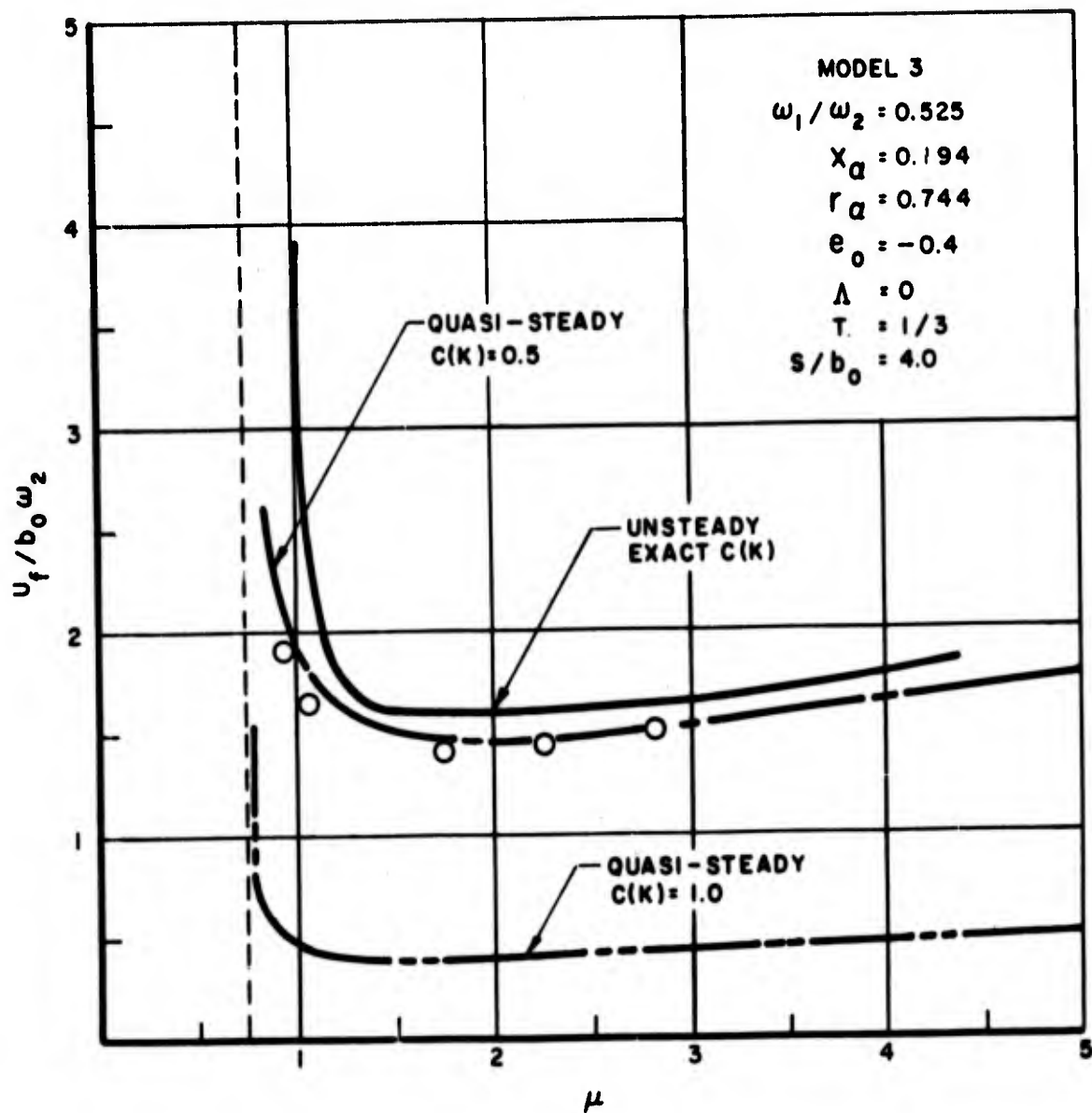
FIGURE 8. COMPARISON OF UNSTEADY, QUASI-STEADY AND EXPERIMENTAL FLUTTER SPEEDS FOR A TWO-DEGREE-OF-FREEDOM HYDROFOIL MODEL IN TWO DIMENSIONAL FLOW

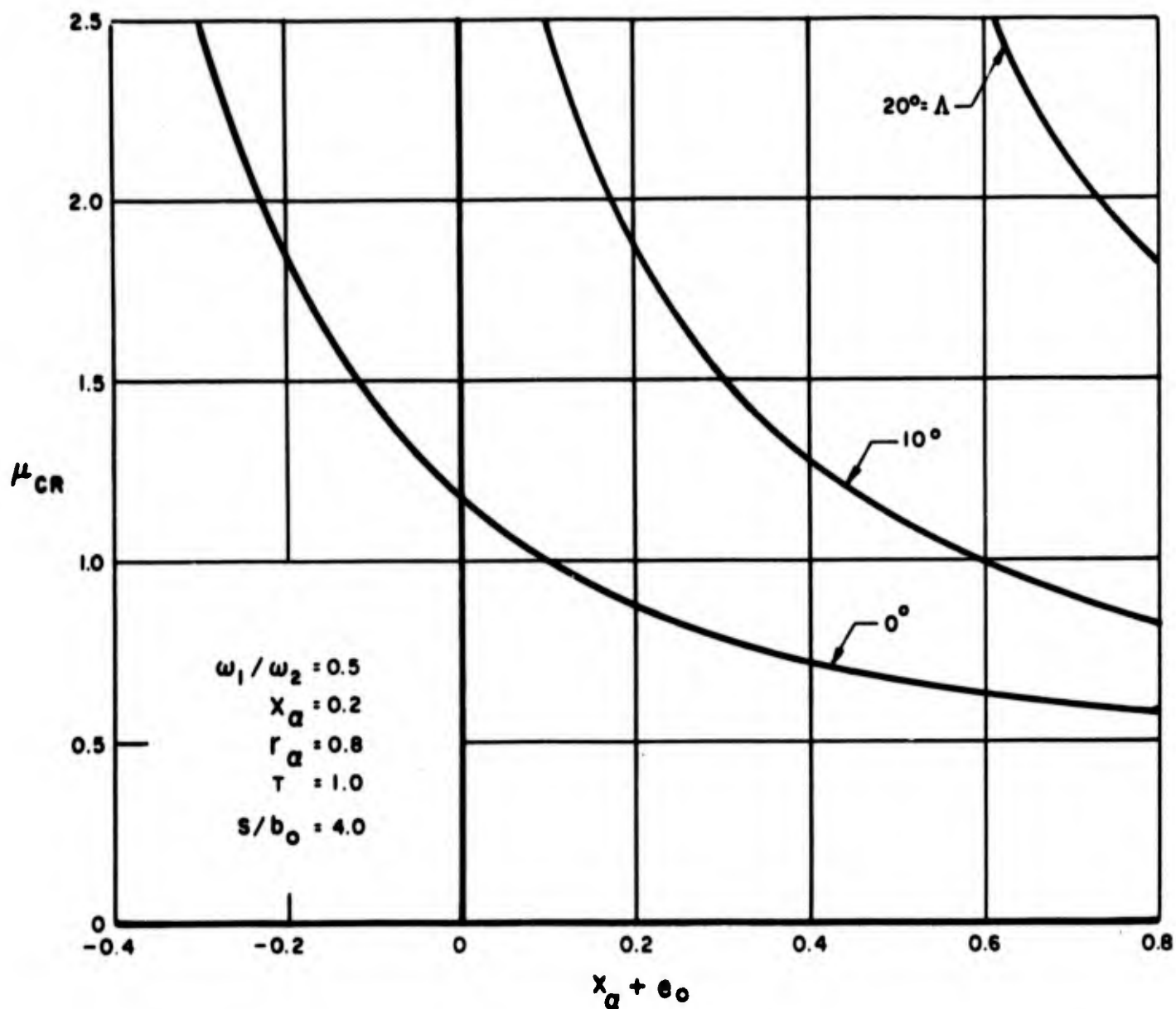FIGURE 9. EFFECT OF SWEEP ANGLE ON FLUTTER SPEED FOR A TWO-DEGREE-OF-FREEDOM HYDROFOIL AS PREDICTED BY TWO-DIMENSIONAL STRIPWISE TECHNIQUE

FIGURE 10. EFFECT OF SWEEP ON CRITICAL DENSITY RATIO FOR A TWO–DEGREE–OF–FREEDOM HYDROFOIL MODEL IN TWO–DIMENSIONAL FLOW
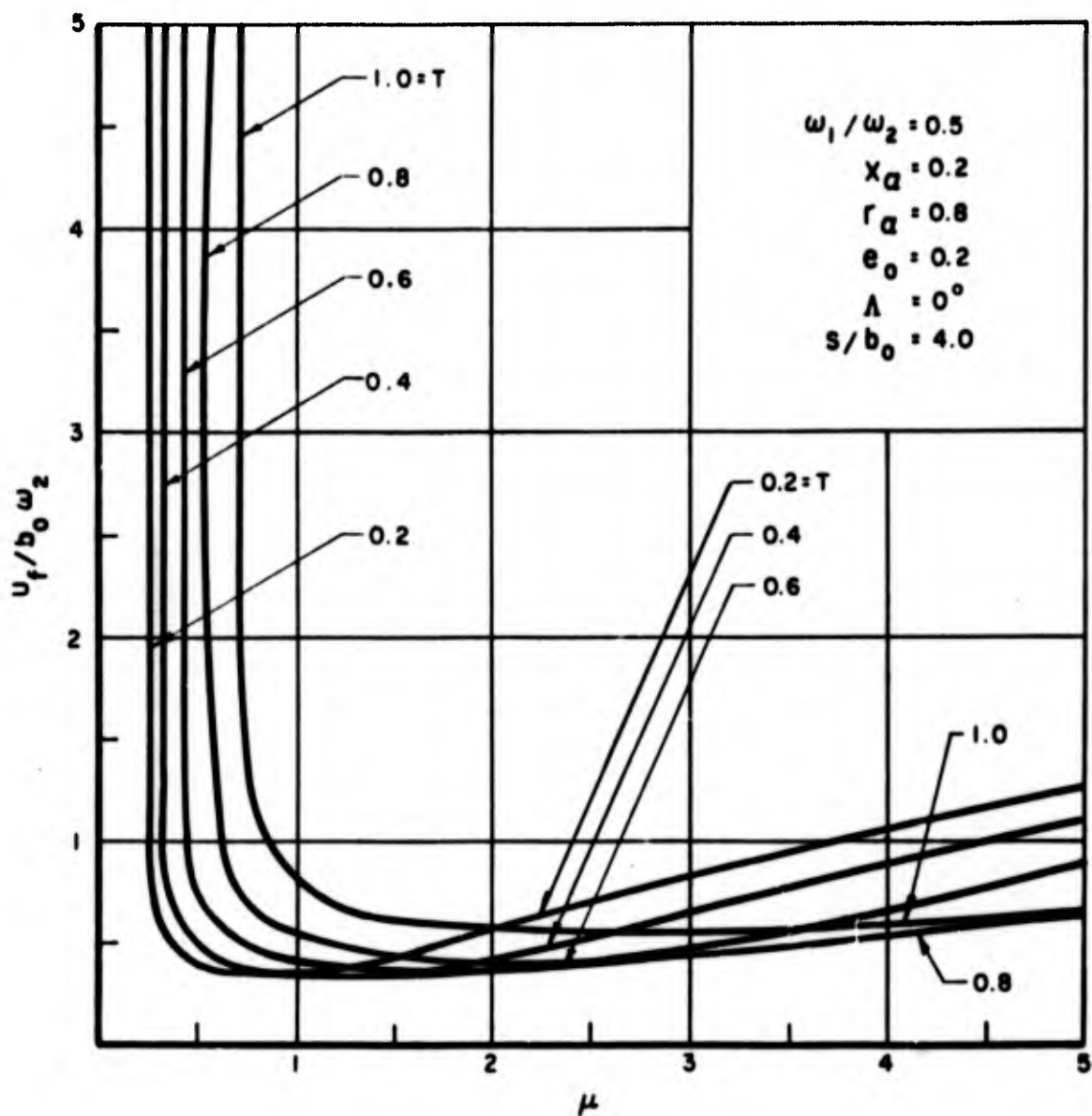
FIGURE II. EFFECT OF TAPER RATIO ON FLUTTER SPEED FOR A TWO-DEGREE-OF-FREEDOM HYDROFOIL AS PREDICTED BY TWO-DIMENSIONAL STRIPWISE TECHNIQUE
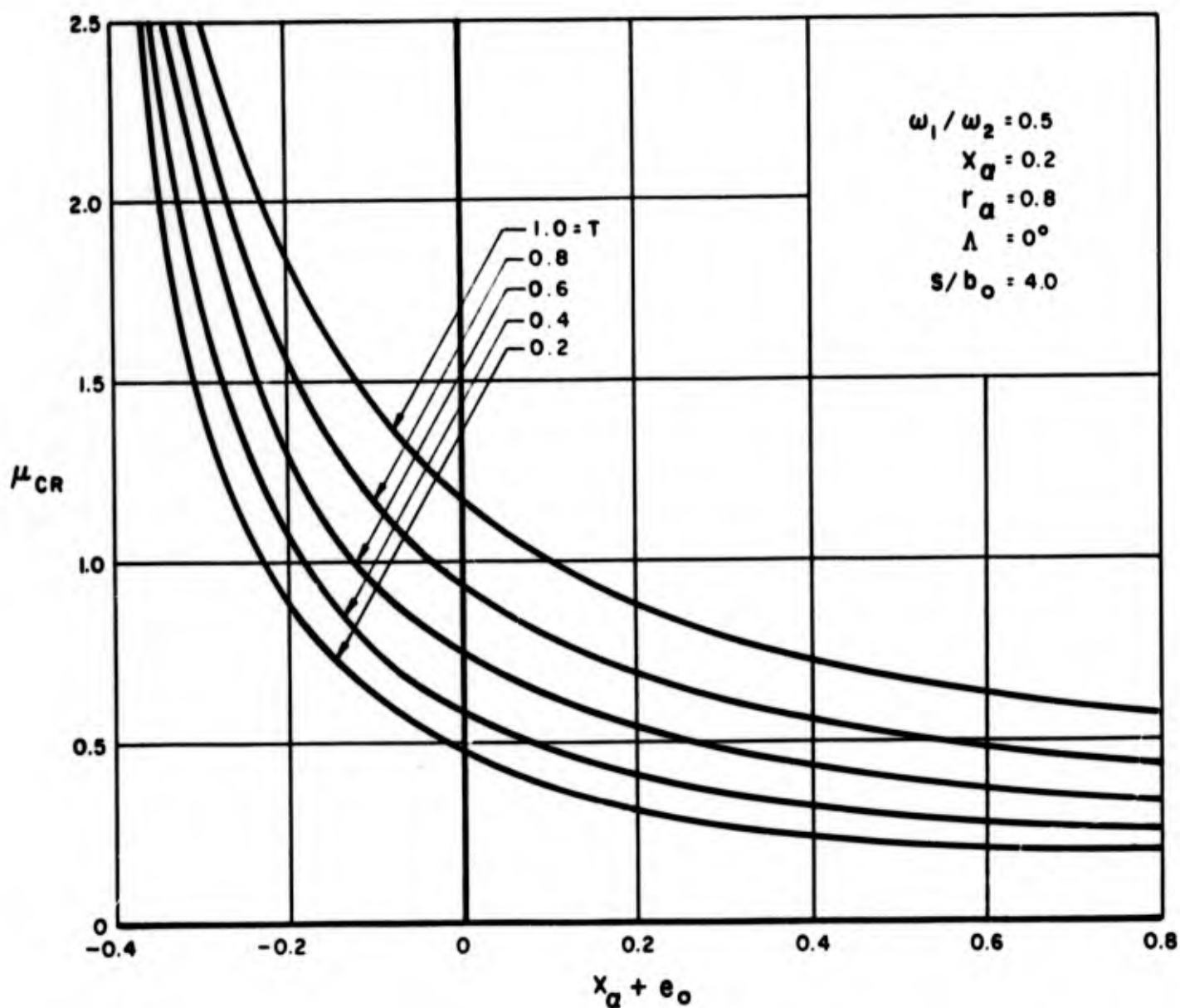
FIGURE 12.   EFFECT OF TAPER ON CRITICAL DENSITY RATIO FOR A
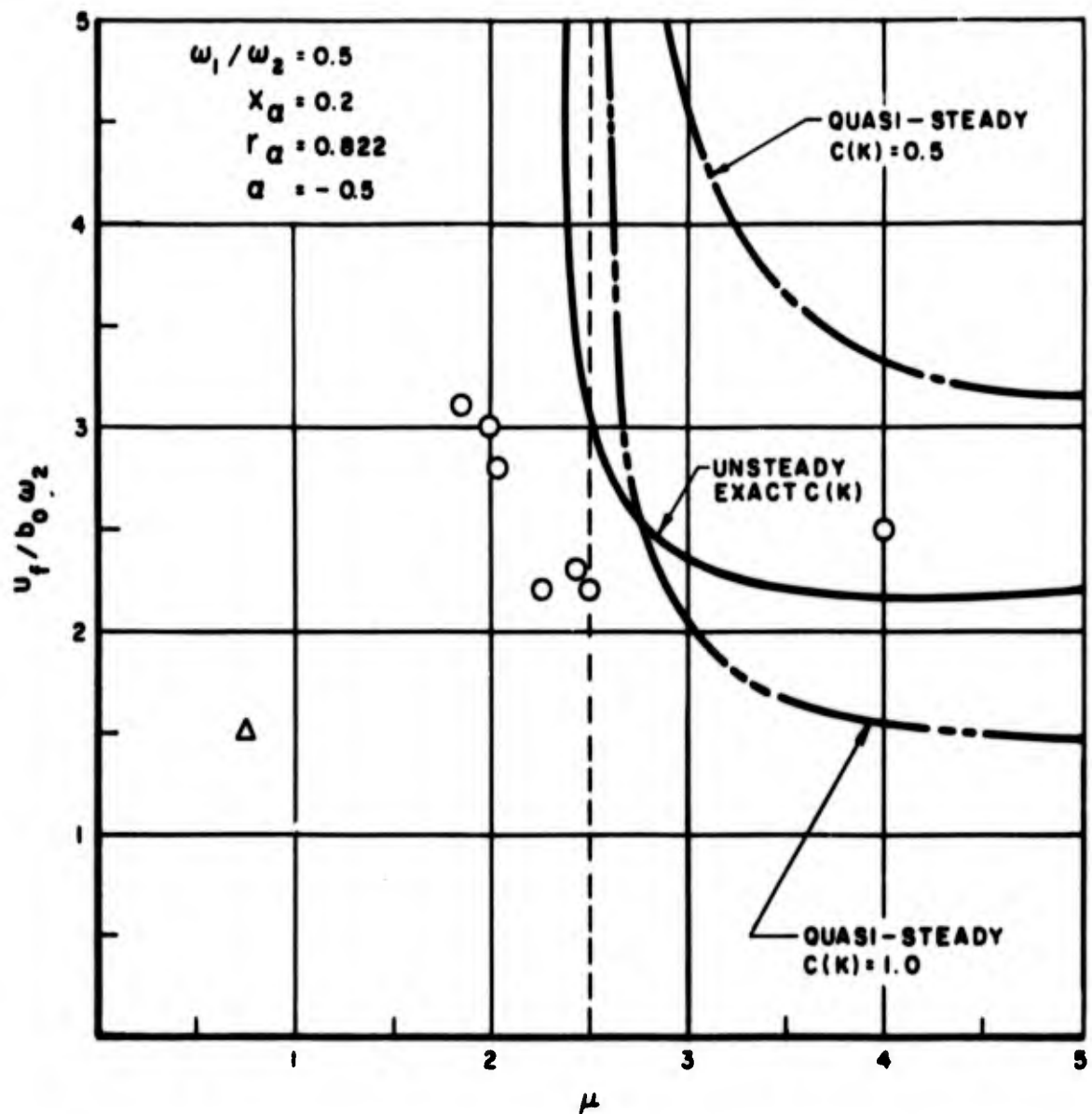TWO-DEGREE-OF-FREEDOM HYDROFOIL MODEL IN TWO-
DIMENSIONAL FLOW

FIGURE 13.   COMPARISON OF UNSTEADY, QUASI-STEADY AND
EXPERIMENTAL FLUTTER SPEEDS FOR-TWO-DEGREE-
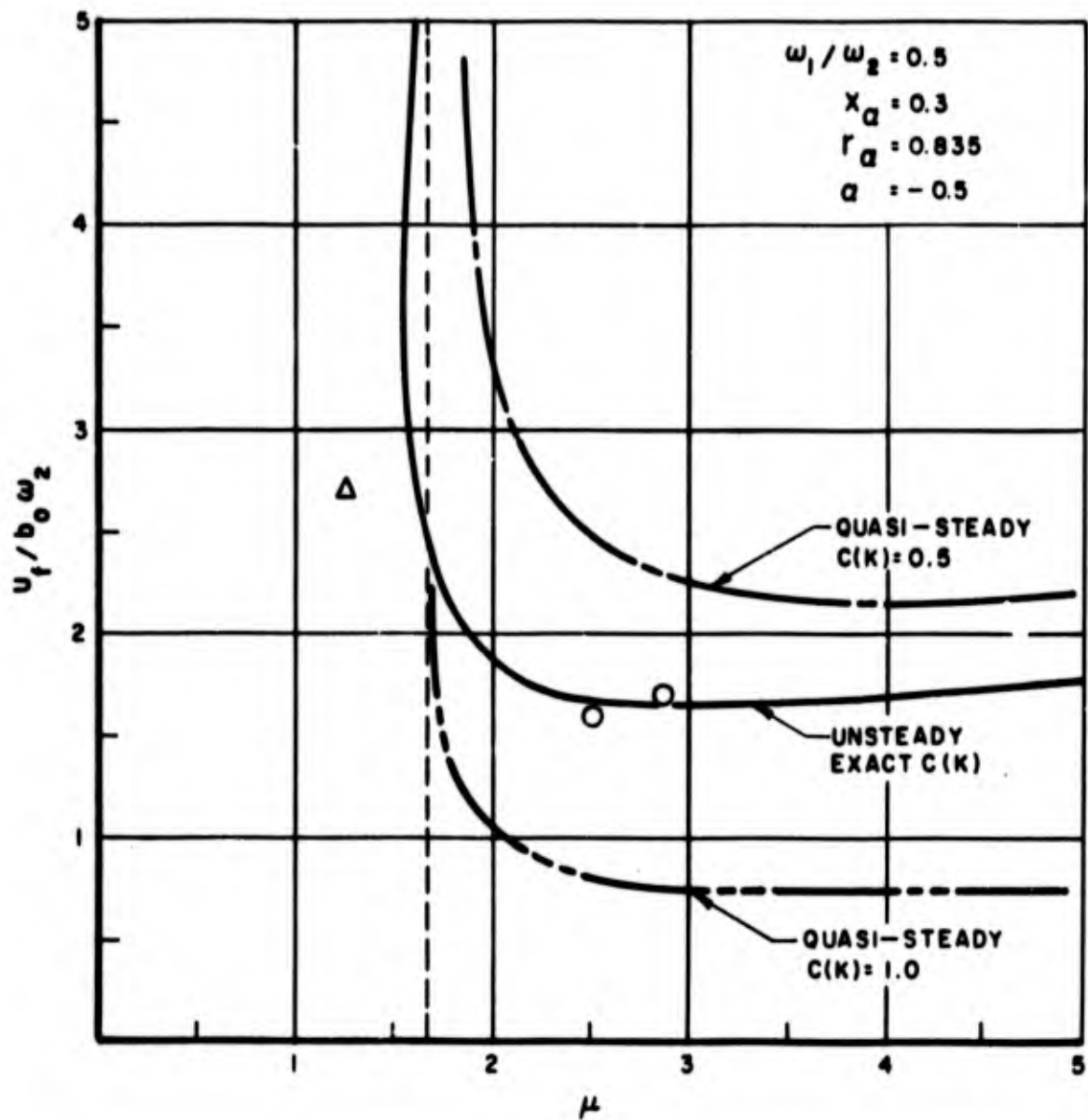OF-FREEDOM HYDROFOIL IN TWO-DIMENSIONAL FLOW

FIGURE 14.   COMPARISON OF UNSTEADY, QUASI-STEADY AND
EXPERIMENTAL FLUTTER SPEEDS FOR TWO-DEGREE-
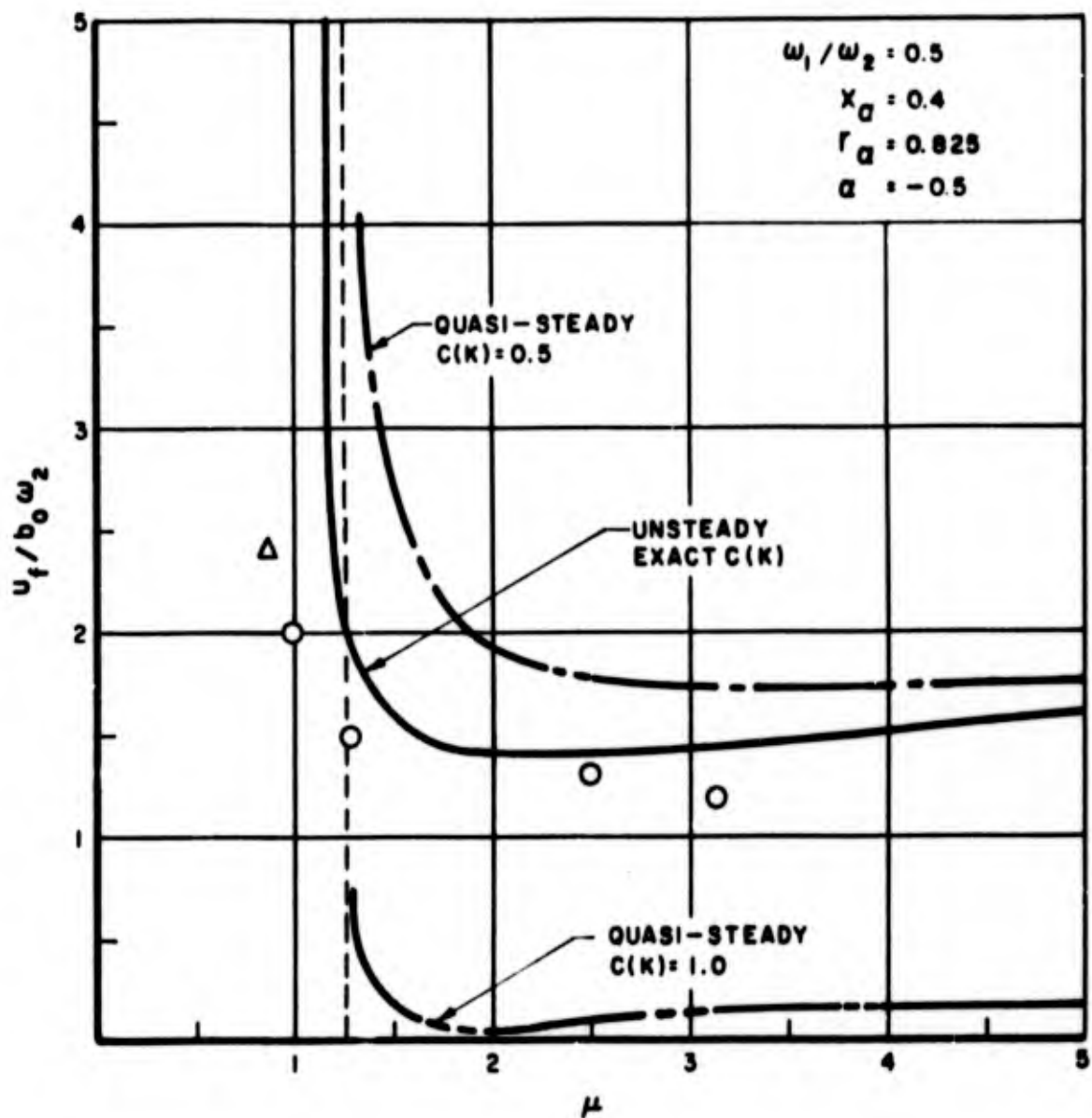OF-FREEDOM HYDROFOIL IN TWO-DIMENSIONAL FLOW

FIGURE 15. COMPARISON OF UNSTEADY, QUASI-STEADY AND
EXPERIMENTAL FLUTTER SPEEDS FOR TWO-DEGREE-
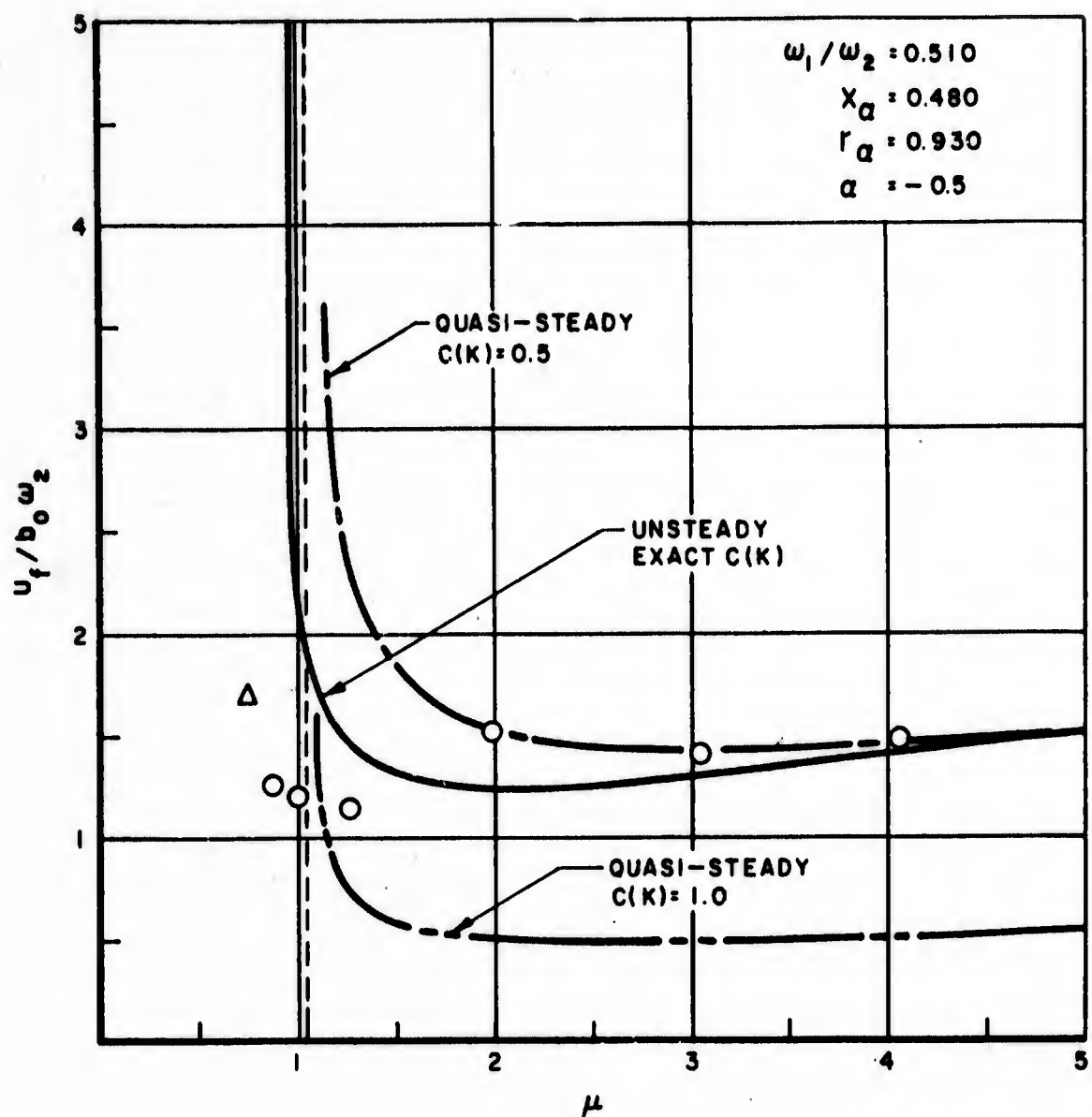OF-FREEDOM HYDROFOIL IN TWO-DIMENSIONAL FLOW

FIGURE 16.   COMPARISON OF UNSTEADY, QUASI-STEADY AND
EXPERIMENTAL FLUTTER SPEEDS FOR A TWO-DEGREE-
OF-FREEDOM HYDROFOIL MODEL IN TWO DIMENSIONAL
FLOW

APPENDIX

HARMONIC HYDRODYNAMIC DERIVATIVES
AS GIVEN BY
TWO-DIMENSIONAL STRIPWISE TECHNIQUE
FOR THE CASE OF
TWO DEGREES OF FREEDOM

J = 1 : Translation   J = 2 : Rotation

$$\frac{\overline{Q}_1}{\pi \rho b_0^3 \omega^2 s} = \frac{\overline{q}_1}{b_0}\left(F_{hr} - \frac{1}{k_0}F_{hi}\right) + \overline{q}_2\left(F_{\alpha r} + \frac{F_{\alpha r}'}{k_0^2} - \frac{1}{k_0}F_{\alpha i}\right)$$

$$\frac{\overline{Q}_2}{\pi \rho b_0^4 \omega^2 s} = \frac{\overline{q}_1}{b_0}\left(T_{hr} - \frac{1}{k_0}T_{hi}\right) + \overline{q}_2\left(T_{\alpha r} + \frac{T_{\alpha r}'}{k_0^2} - \frac{1}{k_0}T_{\alpha i}\right)$$

$$C(k) = \text{Theodorsen function} = F(k) + iG(k)$$

$$F_{hr} = \int_0^1 \left(\frac{b}{b_0}\right)^2 \left[1 + \frac{2G(k)}{k}\right] d\frac{y}{s} \cos\Lambda$$

$$F_{hi} = \int_0^1 \left(\frac{b}{b_0}\right) 2F(k) \, d\frac{y}{s} \cos\Lambda$$

$$F_{\alpha r} = \int_0^1 \left(\frac{b}{b_0}\right)^3 \left[a - \frac{2G(k)}{k}\left(\tfrac{1}{2} - a\right)\right] d\frac{y}{s} \cos\Lambda$$

$$F_{\alpha r}' = F_{hi}$$

$$F_{\alpha i} = -\int_0^1 \left(\frac{b}{b_0}\right)^2 \left[1 + 2F(k)\left(\tfrac{1}{2} - a\right) + \frac{2G(k)}{k}\right] d\frac{y}{s} \cos\Lambda$$

$$T_{hr} = \int_0^1 \left(\frac{b}{b_0}\right)^3 \left[a + \frac{2G(k)}{k}\left(\tfrac{1}{2} + a\right)\right] d\frac{y}{s} \cos \Lambda$$

$$T_{hl} = \int_0^1 \left(\frac{b}{b_0}\right)^3 2F(k)\left(\tfrac{1}{2} + a\right) d\frac{y}{s} \cos \Lambda$$

$$T_{\alpha r} = \int_0^1 \left(\frac{b}{b_0}\right)^4 \left[\tfrac{1}{8} + a^2 - \frac{2G(k)}{k}\left(\tfrac{1}{4} - a^2\right)\right] d\frac{y}{s} \cos \Lambda$$

$$T_{\alpha r}' = T_{hl}$$

$$T_{\alpha l} = \int_0^1 \left(\frac{b}{b_0}\right)^3 \left[\tfrac{1}{2} - a - 2F(k)\left(\tfrac{1}{4} - a^2\right) - \frac{2G}{\kappa^2}\left(\tfrac{1}{2} + a\right)\right] d\frac{y}{s} \cos \Lambda$$

DOCUMENT CONTROL DATA - R&D

(Security classification of title, body of abstract and indexing annotation must be entered when the overall report is classified)

1. ORIGINATING ACTIVITY (Corporate author)	2a. REPORT SECURITY CLASSIFICATION
DAVIDSON LABORATORY, Stevens Institute of Technology	Unclassified
	2b GROUP

3. REPORT TITLE

HYDROFOIL FLUTTER PHENOMENON AND AIRFOIL FLUTTER THEORY; Vol. III, Sweep and Taper

4. DESCRIPTIVE NOTES *(Type of report and inclusive dates)*
Final

5. AUTHOR(S) *(Last name, first name, initial)*

Henry, Charles, J. and Ali, M. Raihan

6. REPORT DATE	7a. TOTAL NO. OF PAGES	7b. NO. OF REFS
December 1965	64	14

8a. CONTRACT OR GRANT NO.	9a. ORIGINATOR'S REPORT NUMBER(S)
NObs 88365, Task 1719	R-1115
b. PROJECT NO. DL Project 2709/227	
c.	9b. OTHER REPORT NO(S) (Any other numbers that may be assigned this report)
d.	

10. AVAILABILITY/LIMITATION NOTICES

Qualified requesters may obtain copies of this report from DDC.

11. SUPPLEMENTARY NOTES	12. SPONSORING MILITARY ACTIVITY
	Bureau of Ships, Dept. of the Navy

13. ABSTRACT

Measured decay rates and flutter speeds for a two-degree-of-freedom hydrofoil model with sweep or taper do not agree with the decay rates and flutter speeds predicted by two-dimensional strip theory, whereas the measured and predicted frequencies are in agreement. Calculations based on the two-dimensional strip theory show that increasing sweep angle or decreasing taper yields higher flutter speeds as well as higher values of the critical density ratio. It is shown that flutter-speed predictions based on quasi-steady representations of the unsteady hydrodynamic forces are not valid.

14. KEY WORDS	LINK A		LINK B		LINK C	
	ROLE	WT	ROLE	WT	ROLE	WT
Hydroelasticity						
Flutter						

INSTRUCTIONS

1. ORIGINATING ACTIVITY: Enter the name and address of the contractor, subcontractor, grantee, Department of Defense activity or other organization (corporate author) issuing the report.

2a. REPORT SECURITY CLASSIFICATION: Enter the overall security classification of the report. Indicate whether "Restricted Data" is included. Marking is to be in accordance with appropriate security regulations.

2b. GROUP: Automatic downgrading is specified in DoD Directive 5200.10 and Armed Forces Industrial Manual. Enter the group number. Also, when applicable, show that optional markings have been used for Group 3 and Group 4 as authorized.

3. REPORT TITLE: Enter the complete report title in all capital letters. Titles in all cases should be unclassified. If a meaningful title cannot be selected without classification, show title classification in all capitals in parenthesis immediately following the title.

4. DESCRIPTIVE NOTES: If appropriate, enter the type of report, e.g., interim, progress, summary, annual, or final. Give the inclusive dates when a specific reporting period is covered.

5. AUTHOR(S): Enter the name(s) of author(s) as shown on or in the report. Enter last name, first name, middle initial. If military, show rank and branch of service. The name of the principal author is an absolute minimum requirement.

6. REPORT DATE: Enter the date of the report as day, month, year; or month, year. If more than one date appears on the report, use date of publication.

7a. TOTAL NUMBER OF PAGES: The total page count should follow normal pagination procedures, i.e., enter the number of pages containing information.

7b. NUMBER OF REFERENCES: Enter the total number of references cited in the report.

8a. CONTRACT OR GRANT NUMBER: If appropriate, enter the applicable number of the contract or grant under which the report was written.

8b, 8c, & 8d. PROJECT NUMBER: Enter the appropriate military department identification, such as project number, subproject number, system numbers, task number, etc.

9a. ORIGINATOR'S REPORT NUMBER(S): Enter the official report number by which the document will be identified and controlled by the originating activity. This number must be unique to this report.

9b. OTHER REPORT NUMBER(S): If the report has been assigned any other report numbers (either by the originator or by the sponsor), also enter this number(s).

10. AVAILABILITY/LIMITATION NOTICES: Enter any limitations on further dissemination of the report, other than those imposed by security classification, using standard statements such as:

(1) "Qualified requesters may obtain copies of this report from DDC."

(2) "Foreign announcement and dissemination of this report by DDC is not authorized."

(3) "U. S. Government agencies may obtain copies of this report directly from DDC. Other qualified DDC users shall request through

_____."

(4) "U. S. military agencies may obtain copies of this report directly from DDC. Other qualified users shall request through

_____."

(5) "All distribution of this report is controlled. Qualified DDC users shall request through

_____."

If the report has been furnished to the Office of Technical Services, Department of Commerce, for sale to the public, indicate this fact and enter the price, if known.

11. SUPPLEMENTARY NOTES: Use for additional explanatory notes.

12. SPONSORING MILITARY ACTIVITY: Enter the name of the departmental project office or laboratory sponsoring (paying for) the research and development. Include address.

13. ABSTRACT: Enter an abstract giving a brief and factual summary of the document indicative of the report, even though it may also appear elsewhere in the body of the technical report. If additional space is required, a continuation sheet shall be attached.

It is highly desirable that the abstract of classified reports be unclassified. Each paragraph of the abstract shall end with an indication of the military security classification of the information in the paragraph, represented as (TS), (S), (C), or (U).

There is no limitation on the length of the abstract. However, the suggested length is from 150 to 225 words.

14. KEY WORDS: Key words are technically meaningful terms or short phrases that characterize a report and may be used as index entries for cataloging the report. Key words must be selected so that no security classification is required. Identifiers, such as equipment model designation, trade name, military project code name, geographic location, may be used as key words but will be followed by an indication of technical context. The assignment of links, roles, and weights is optional.

DD FORM 1473 (BACK)
1 JAN 64